Brain Pathology 8: 195-215(1998)

Mouse Models of Human Lysosomal Diseases

Kinuko Suzuki[1,3], Richard L. Proia[2], and Kunihiko Suzuki[3,4]

[1] Department of Pathology and Laboratory Medicine , University of North Carolina, Chapel Hill (NC)
[2] Genetics and Biochemistry Branch, National Institute of Diabetes and Digestive and Kidney Diseases, National Institutes of Health, Bethesda (MD)
[3] Neuroscience Center, University of North Carolina, Chapel Hill (NC)
[4] Departments of Neurology and Psychiatry, University of North Carolina, Chapel Hill (NC), USA

Genetically authentic animal models of human lysosomal diseases occur spontaneously in many mammalian species. However, most are among larger domestic or farm animals with only two well-defined genetic lysosomal diseases known among rodents. This status changed dramatically in recent years with the advent of the combined homologous recombination and embryonic stem cell technology, which allows directed generation of mouse models that are genetically equivalent to human diseases. Almost all known human sphingolipidoses, two mucopolysaccharidoses and aspartylglycosaminuria have so far been duplicated in mice and more are expected in the near future. This technology also allows generation of mouse mutants that are not known or are highly unlikely to exist in humans, such as "double-knockouts." These animal models will play an important role in studies of the pathogenesis and treatment of these disorders. While the utility of these mouse models is obvious, species differences in brain development and metabolic pathways must be always remembered, if the ultimate goal of the study is application to human patients.

Corresponding author:
Kinuko Suzuki, MD, Department of Pathology and Laboratory Medicine, Neuroscience Center, University of North Carolina, Chapel Hill, NC 27599-7525, USA, Tel.: +1-919-966 4584; Fax: +1-919-966 6718; E-mail: KIS@MED.UNC.Edu

Introduction

Lysosomal storage disorders are a group of diseases caused by the deficient activity of individual lysosomal enzymes. Typically the diseases involve the central as well as peripheral nervous system. Defective genes have been identified in the majority of these diseases and large numbers of mutations are identified. Naturally occurring animal models of lysosomal storage diseases have been identified during the past decades and have been used for the investigation of basic pathogenesis as well as exploration of therapeutic approaches (1, 2, 26, 32, 59, 72, 85, 86, 94, 95). However, the availability of such naturally occurring models, and in particular small animal models, is very limited.

With recent advances in DNA recombinant technology and in knowledge of mouse reproductive biology, many mouse models of human diseases have been generated by targeted disruption of specific genes. At this time of writing at the middle of 1997, at least 14 mouse models of human lysosomal diseases have been published and one documented in an abstract form (Table 1), and the numbers most certainly will increase rapidly. Obviously the mouse is not a human being and thus significant phenotypic differences may exist between the diseases of these two species. In this review we focused our description on the clinical phenotype, biochemical characteristics and pathological features of the specific human diseases and those of transgenic mouse models generated by targeted gene disruption (knockout mice). Those who are interested in technical details of generating these knockout mice are referrered to the original articles listed as references.

Gaucher disease

Gaucher disease is an autosomal recessive disease caused by a deficient activity of the lysosomal hydrolase, glucosylceramidase (or glucocerebrosidase), resulting in massive accumulation of glucocerebroside in cells of the reticuloendothelial system. These storage cells, Gaucher cells, are found throughout the visceral tissues and result in hepatosplenomegaly, the most conspicuous clinical feature in human patients. Traditionally Gaucher disease is classified into three clinical forms. Type I is a non-neuronopathic form affecting mostly

Inactivated gene	Equivalent human disease
Naturally occurring models	
Galactosylceramidase (Twitcher mouse)	Krabbe disease
β-glucuronidase	MPS VII
Transgenic (knockout) mouse models	
Glucosylceramidase	Gaucher disease
β-Hexosaminidase α-subunit	Tay-Sachs disease
β-Hexosaminidase β-subunit	Sandhoff disease
G_{M2} activator	G_{M2} gangliosidosis AB variant
β-Hexosaminidase α- and β-subunit	Unknown
β-Galactosidase	G_{M1} gangliosidosis
β-gal/sialidase Protective protein	Galactosialidosis
Sphingomyelinase	Niemann-Pick disease type A and B
α-galactosidase A	Fabry disease
Arylsulfatase A (sulfatidase)	Metachromatic Leukodystrophy
Sphingolipid activator (prosaposin) deficiency	Total sphingolipid activator deficiency
α-L-iduronidase	Hurler-Scheie (MPS IH and IS)
Arylsulfatase B	Maroteaux-Lamy (MPS VI)
glycosylasparaginase	Aspartylglucosaminuria
N-acetyl α-galactosaminidase*	Schindler disease

*Abstract only (87)

Table 1. Mouse models of lysosomal disease.

adults, type II is a severe infantile neuronopathic form and type III is termed subacute neuronopathic or juvenile form and is a phenotypically intermediate type. Type I is highly prevalent in the Ashkenazi Jewish population, and a distinct group of type III patients exist in Scandinavian countries. No ethnic predilection is known for the type II disease (5). Gaucher cells were detected in the brain of type II patients and to a lesser extent in type III patients, in association with marked neuronal degeneration. In addition, a rapidly progressing fulminating phenotype in neonates, a subtype of type II Gaucher disease, was recognized recently. This type closely resembles the mouse model generated by targeted disruption of glucosylceramidase gene described below (68). All types are allelic and the gene for glucosylceramidase is located on chromosome 1 in the region of q21. Many point mutations in the glucosylceramidase gene have been identified in Gaucher patients (5).

Mouse model. In 1992, Tybulewicz and co-workers (82) generated a murine model for Gaucher disease by creating a null allele in embryonic stem cells through gene targeting and using these genetically modified cells to establish a mouse strain carrying the mutation. To disrupt the murine glucocerebrosidase gene, the neomycine-resistance (Neo) gene was inserted into exons 9 and 10, which encode part of the active site of the enzyme. The targeted mutation was transmitted in Mendelian fashion. The glucosylceramidase activity in these homozygous mutant mice was less than 4% of control. Increased amounts of glucocerebroside was demonstrated in the mutant tissue (liver, lung, brain and bone marrow). The homozygous mutant mice, however, were akinetic with irregular respiration and poor feeding, and died within 24 hours of birth with rapidly progressing cyanosis. Tybulewicz and co-workers have studied over 100 homozygous mice. No typical Gaucher cells were observed at the light microscope level in any of the tissues that showed increased glucocerebroside, although with electron microscopic studies the stored lipid, that had the same physical appearance as the inclusions found in cells of the Gaucher patients, was identified in the macrophages in the liver, spleen and bone marrow of the homozygous mice. However, the extent of glucocerebroside accumulation in the organs did not appear to be sufficient to explain the rapid deterioration in these newborn mutant mice. In the CNS, no Gaucher cells were observed although tubular Gaucher type inclusions were identified in microglia and neurons of the red nucleus and vestibular nucleus, sensory and motor neurons at the ultrastructural level (89). These mice did not show any hepatosplenomegaly or infiltration of Gaucher cells in the brain as noted in human cases. The most significant pathology in these mice was noted in the skin. Their skin showed abnormally prominent rugation and hyperkeratosis. These feature were nearly identical to those of a severe subtype of type II Gaucher disease, (“collodion” babies, or Gaucher infants having congenital ichthyosis or “cellophane like” skin) (68). Ceramide has been demonstrated to play an important role in skin permeability barrier homeostasis. The absence of glucosylceramidase may consequently affect functional skin integrity, since elimination of glucocerebroside and accumulation of ceramides occur during the maturational process in membrane structure establishing a permeability barrier. Thus, the enzyme deficiency with resultant abnormal glucocerebroside degradation appeared directly responsible for the abnormal skin of this subtype of Gaucher infants and mutant mice. Histologically, the thickened overlying keratin layer was found in the skin of both the homozygous mutant mice and neonatal Gaucher patients. During the final stages of epidermal differentiation, extrusion of lamellar body contents (at the stratum granulosum/stratum corneum interface) is followed sequentially by unfurling, elongation, and processing into a mature lamellar bilayer unit structure. However, in the mutant mice, ultrastructural abnormalities including the persistence of incompletely processed lamellar body-derived content, indicating perturbed maturation, was demonstrated throughout the striatum corneum interstices. Furthermore, these mice demonstrated

markedly elevated transepidermal water loss as well as altered permeability barrier function as shown by an electron dense tracer study (31). Such changes were not detected in the skin of type I or III Gaucher patients (67).Thus, phenotypically these model mice resemble a rare but the most severe subtype of type II Gaucher disease.

Gangliosidoses

Gangliosidoses are autosomal recessive lysosomal storage diseases caused by abnormal metabolism of tissue gangliosides, sialic acid-containing sphingolipids. Two groups, G_{M1} gangliosidosis and G_{M2} gangliosidosis, are known in humans. Naturally occurring feline and canine models of gangliosidoses have been widely used for investigations of pathogenesis as well as therapeutic strategies (1, 3, 46, 85).

G_{M2} gangliosidoses

G_{M2} gangliosidoses are caused by a deficient activity of β-hexosaminidase or G_{M2} activator protein. Three distinct polypeptides, the β-hexosaminidase α and β-subunits and the G_{M2} activator protein are involved in normal degradation of G_{M2} ganglioside in vivo (Figure 1). Three dimeric forms of β-hexosaminidase exist; hexosaminidase A is a heterodimer consisting of α and β subunits (αβ) and hexosaminidase B is a homodimer consisting of two β subunits (ββ). The minor form, hexosaminidase S, is an αα homodimer (αα). The gene for the β-hexosaminisase α subunit (*HEXA*) is located on chromosome 15, while genes for β subunit (*HEXB*) and for G_{M2} activator (GM2A) are on chromosome 5 (Figure 1). Thus, deletion or mutation of these genes causes three types of G_{M2} gangliosidoses; hexosaminidase A and S deficiency (Tay-Sachs disease), hexosaminidase A and B deficiency (Sandhoff disease) and G_{M2} activator deficiency (AB variant). Their clinical phenotypes are very similar. Deficiency in activity of hexosaminidase or G_{M2} activator results in massive accumulation of G_{M2} ganglioside and other glycolipids in neuronal lysosomes. These glycolipids are stored as multilamellar structures known as membranous cytoplasmic bodies (MCBs) (78, 79). In Sandhoff disease, the additional absence of β-hexosaminidase B results in accumulation of other substrates such as G_{A2}, globoside, oligosaccharides and glycosaminoglycans in the visceral organs. The infantile forms are rapidly progressive, resulting in death in early childhood. The late onset forms that usually retain low but detectable level of enzyme activity, progress more slowly with a spectrum of clinical pheno-

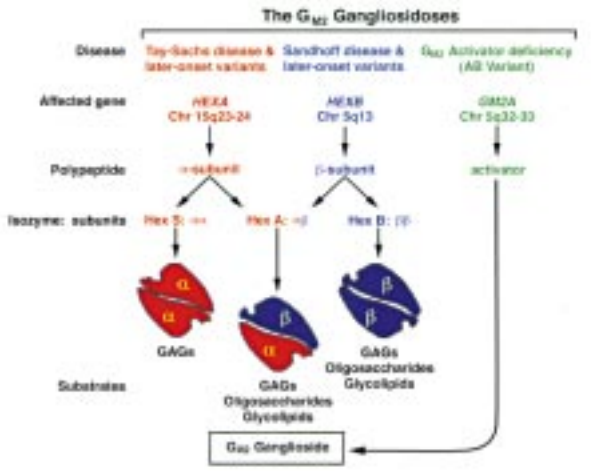

Figure 1. The G_{M2} gangliosidoses and the β-hexosaminidase system. The information provided is for the human β-hexosaminidase system although extensive similarities exist with the mouse system.

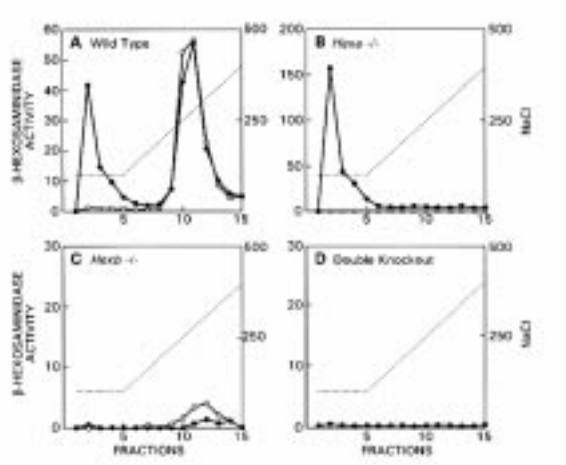

Figure 2. β-hexosaminidase activity in G_{M2} gangliosidosis mice. Liver extracts (2 mg protein) from wild-type **A.**, *Hexa*-/- **B.**, *Hexb*-/- **C.** and double knockout mice **D.** were subjected to ion-exchange chromatography on a Mono Q column. The fractions collected were assayed for β-hexosaminidase activity (nmol substrate cleaved/hr) with the neutral substrate, 4-methylumbelliferyl-2-acetamido-2-deoxy-β-D-glucopyranoside (filled circles) and with the sulfated substrate, 4-methylumbelliferyl-6-sulfo-2-acetamido-2-deoxy-β-glucopyranoside (open circles). The NaCl concentration (mM) gradient is indicated by the dotted line. In wild type **A.** and *Hexa*-/- **B.** mice, the activity eluting in fraction 2-5 represents β-hexosaminidase B. In wild-type mice (A), the activity eluting in fraction 9-14 is primarily β-hexosaminidase A (with, presumably, a small β-hexosaminidase S component). In *Hexb*-/- mice **C.**, the activity eluting in fractions 10-15 represents β-hexosaminidase S. No hexosaminidase activities are found in the double knockout mice **D.**. Note the expansion of β-hexosaminidase activity axis in **C.** and **D.**.

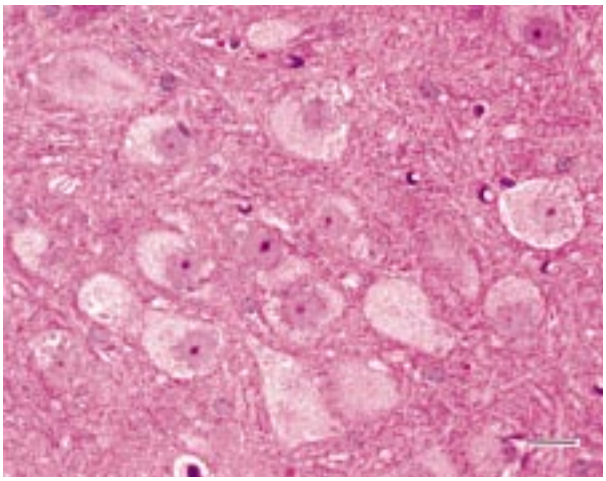

Figure 3. Neurons in the amygdala in *Hexa*-/- mice. The neuronal perikarya are markedly swollen with storage material. The light microscopic feature of the storage neurons are the same in all three types of G_{M2} gangliosidosis mice (*Hexa*-/-, *Hexb*-/- and *Gm2a*-/-).
Solochrome and Eosin stain. Bar 15μm

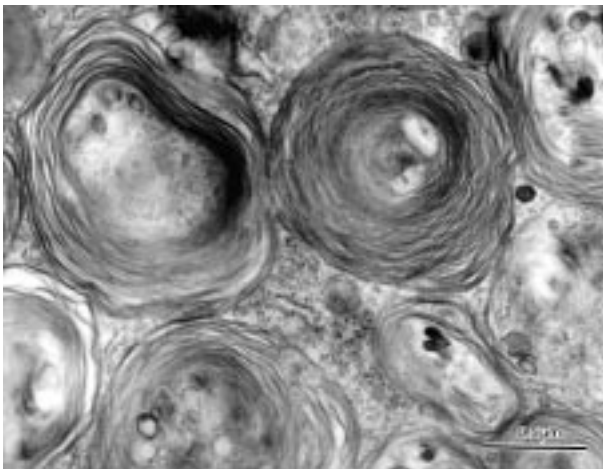

Figure 4. An electronmicrograph of the storage material forming membranous cytoplasmic bodies (MCBs) in the neuronal perikarya. MCBs in these G_{M2} gangliosidosis mice are identical to those of infantile G_{M2} gangliosidosis.

types (21, 74).

Mouse models. In the mouse hexosaminidase system, hexosaminidase A and B are also the major isozymes. Both cDNA for α and β subunits were found to have 84% and 75% identity with their human counterparts in their predicted protein sequences (4, 6, 92) Through targeted disruption of the mouse *Hexa*, *Hexb* and *Gm2a* genes (corresponding to human *HEXA*, *HEXB* and *GM2A* genes) by homologous recombination, we and others have generated mouse models of human G_{M2} gangliosidoses (13, 39, 53, 61, 77, 91).

Tay-Sachs mice. To disrupt the *Hexa* gene, the Neo cassette was introduced into exon 8. The construct was introduced into the embryonic stem cells and heterozygous mice carrying targeted mutation were generated. Heterozygous (*Hexa*+/-) mating yielded *Hexa*-/- progeny in the frequency expected from Mendelian genetics. Homozygous mice with a *Hexa* null mutation (*Hexa*-/- mice) were profoundly deficient with β-hexosaminidase A activity (Figure 2) with an accumulation of G_{M2} ganglioside in the brain as noted in Tay-Sachs disease patients. Storage neurons displayed MCBs at the ultrastructural level (Figure 3, 4). Thus, *Hexa*-/- mice showed biochemical as well as pathological features compatible with Tay-Sachs disease in humans. Unlike human patients, however, these *Hexa*-/- mice were phenotypically normal and fertile, and have a normal life span. Even in those older than one year, no behavioral or motor abnormalities were detected. Thin layer chromatography of the ganglioside fraction from the brain of *Hexa*-/- mice revealed only a faint band at 1-day old (<3% of total ganglioside) but the amounts of G_{M2} ganglioside progressively increased with age, representing 15% of total ganglioside at 6 months of age (91). No morphological abnormalities were noted in the liver, spleen and other visceral organs at the light microscope level, although modest lysosomal storage was reported in the hepatocytes at the ultrastructural level by one group (13). Neuronal storage was evident as early as 2 months of age. The localization of storage neurons appeared to be limited to certain regions in the brain such as cerebral cortex, amygdala, piriform cortex, hippocampus, hypothalamus etc (Fig 5, 6). Notably absent was storage in the Purkinje and granular cells in the cerebellar folia and in neurons in the spinal cord. In the cerebral cortex, large pyramidal neurons appeared to show more storage than other cortical neurons. The storage materials were immunostained with antibody to G_{M2} ganglioside (77). Identical distribution of the storage neurons and G_{M2} ganglioside immunoreactivity was reported in the *Hexa*-/- mice generated by Phaneeuf et al (56). However, in the mice reported by Cohen-Tannoundji and co-workers, no storage was noted in hippocampus at 150 days (13). Limited neuronal storage resulting in an apparently normal phenotype in *Hexa*-/- mice can be explained by differences in the G_{M2} ganglioside degradation pathway between in humans and mouse in that mouse sialidase has a more active role in

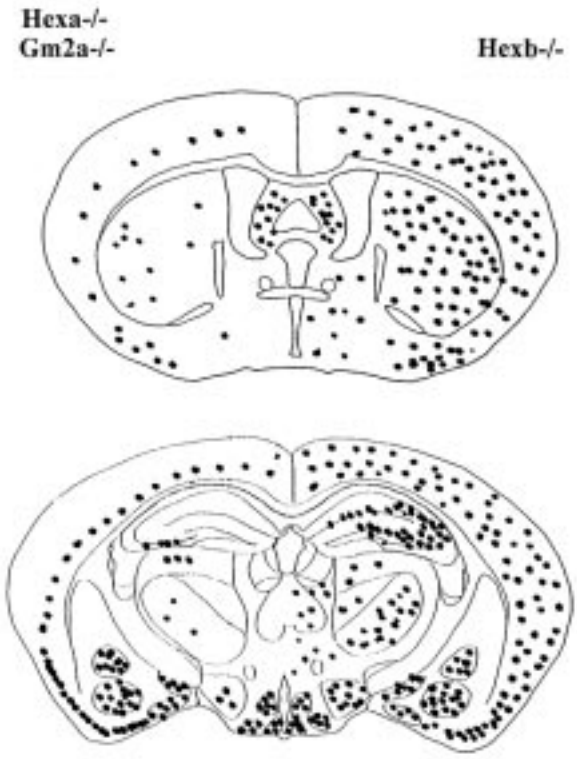

Figure 5. Diagrams showing the distributional pattern of the neuronal storage in *Hexa*-/- *Gm2a*-/- mice and *Hexb*-/- mice.

G_{M2} ganglioside degradation (Figure 7). Although the results obtained with the *Hexa*-/- mice indicate an essential role for β-hexosaminidase A in G_{M2} degradation, even a very low rate of G_{M2} ganglioside degradation by an alternative pathway utilizing β-hexosaminidase B could drastically alter the progression of the storage process (38).

Sandhoff mice. To disrupt the *Hexb* gene, Neo cassette was introduced into exon 13 of the 14 exon *Hexb* gene. Heterozygotes for disrupted *Hexb* gene (*Hexb*-/-) were mated to generate homozygous mice for *Hexb* null mutation (*Hexb*-/-) (61). Liver extracts from *Hexb* knockout mice were deficient in both hexosaminidase A and B activity, containing only about 2% of the wild type hexosaminidase level that most likely corresponded to β-hexosaminidase S (Figure 2). The *Hexb*-/- mice were normal at birth. However, progressive worsening of motor coordination and balance was detected by the rotorod test starting around 12 weeks of age. Generalized locomotion in a Digiscan open field and passive avoidance learning were not significantly different from wild type controls. First signs of severe motor dysfunction became apparent at around 3 months of age. The neurological signs included gait abnormalities with spastic movements starting from hindlimbs and progressing to forelimbs. By 4 to 4.5 months of age, muscle over the hindlimbs became atrophic and the mice were no longer able to take food or water effectively. Both male and female *Hexb*-/- were fertile, however. In the brain of patients with Sandhoff disease, not only G_{M2}

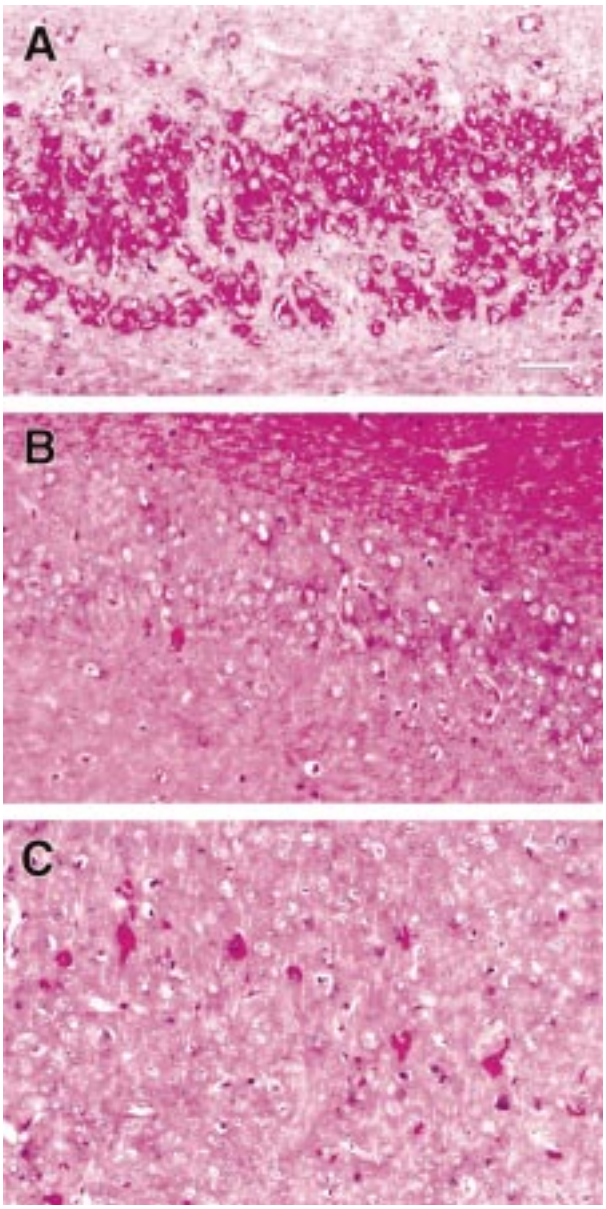

Figure 6. Hippocampal CA3 region of *Hexb*-/- **A.**, *Hexa*-/- **B.** and *Gm2a*-/- **C.** mice. Almost all neurons in *Hexb*-/- are packed with the PAS positive storage material while only sporadic neurons contain PAS positive storage material in *Hexa*-/- and *Gm2a*-/- mice. Frozen sections stained with PAS. Bar 70μm

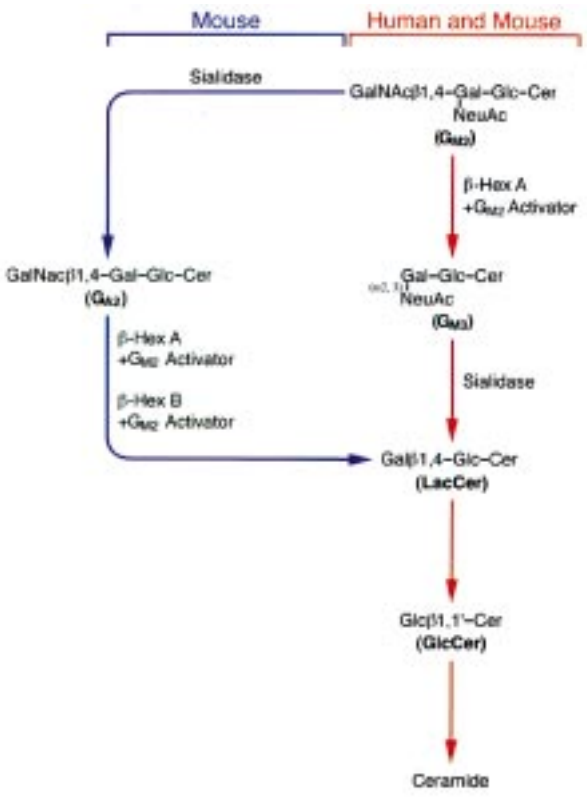

Figure 7. The G_{M2} ganglioside degradation pathway. The hexosaminidase reactions have been established in humans. It is assumed that the murine hexosaminidases have similar specificities based on the glycolipid storage compounds in the brains of *Hexa*-/- and *Hexb*-/- mice. The major degradative pathway in the mouse is in blue. Abbreviations: GlcCer, glucosylceramide; LacCer, lactosylceramide.

ganglioside but its asialo form, glycolipid G_{A2}, accumulate. In the brain of a 41 day old *Hexb*-/- mouse, similar accumulation of both G_{M2} ganglioside and G_{A2} was readily detectable. G_{M2} ganglioside was detected in a 41 day old *Hexa*-/- mouse but was at ¼ the level of the *Hexb*-/- mouse and no G_{A2} was detected. These biochemical differences correspond well with the differences in the extent of neuronal storage noted in these two mouse models. Neither G_{M2} ganglioside nor glycolipid G_{A2} was detectable in the wild type mice. On histological examination, extensive neuronal storage was observed throughout the cerebrum, cerebellum, brainstem, spinal cord, trigeminal and dorsal root ganglia, retina and myenteric plexus. Unlike *Hexa*-/- mice, abundant storage was noted in the Purkinje and granular cell neurons as well as in many cells in the molecular layer of the cerebellum. Storage was also very conspicuous in the spinal neurons. These storage materials were best demonstrated in the frozen section preparation stained with periodic acid Schiff (PAS) stain (Figure 6). In addition to neurons, PAS positive storage materials were noted in small round cells in the cerebrum and cerebellum. The storage materials in these small cells, but not those in neurons, were also stained positively with alcian blue and colloidal iron consistent with glycosaminoglycans. These cells stained positively with a lectin, RCA-1 indicative of macrophage/microglia and tended to be located at the perivascular regions. Similarly PAS and alcian blue/colloidal iron stained cells were noted in the hepatic sinusoids. Epithelial cells of the proximal tubules in the kidney also contained similarly stained materials. These histological features are identical to those of Sandhoff disease in humans. The cerebral white matter was diffusely hypomyelinated compared with the *Hexa*-/- or wild type mice. White matter degeneration with axonal spheroids was recognized in the spinal cord of older mice. Unlike Tay-Sachs and Sandhoff disease in humans, where the clinical course is nearly identical, the corresponding mouse models, *Hexa*-/- and *Hexb*-/- show quite different phenotypes. Clinical as well as pathologic phenotypes of *Hexb*-/- generated by Phaneuf and co-workers (56) were essentially very similar to those generated by Sango and coworkers (61). Axonal degeneration with spheroid formation appeared to be more pronounced in the former, however (56). These phenotypic differences are readily explained by the different extent of the brain pathology, resulting from possible differences in ganglioside degradation pathway in mouse and humans. Analysis of ganglioside degradation pathway in mice and humans with embryonic fibroblasts in culture indicated the presence of an alternate pathway in mice (Figure7). In humans, G_{M2} is degraded, almost exclusively, by β-hexosaminidase A with activator protein to produce G_{M3}. Mice, in addition to this human pathway, have a second pathway where G_{M2} is converted to G_{A2} by the action of sialidase. In Tay-Sachs patients and *Hexa* -/- mice, the conversion of G_{M2} to G_{M3} is blocked by the absence of β-hexosaminidase A. However, in mice the major degradative pathway, the conversion of G_{M2} to G_{A2} by sialidase, remains intact. G_{A2} degradation in the *Hexa*-/- can then be catalyzed by β-hexosaminidase B explaining their limited G_{M2} ganglioside storage and lack of neurologic symptoms. In *Hexb*-/- mice, both pathways are blocked leading to extensive neuronal storage of both G_{A2} and G_{M2} ganglioside and a severe phenotype similar to infantile -onset G_{M2} gangliosidosis in humans. Thus, unlike in humans, β-hexosaminidase B can participate in the G_{M2}

ganglioside degradation pathway in mice (61). The differences in the distribution of neuronal storage between *Hexa*-/- and *Hexb*-/- also suggest regional variation of ganglioside metabolism in the mouse brain.

AB variant mouse. The Gm2a gene was disrupted by a deletion of a portion of exon 3 and all of the coding region of exon 4. Heterozygous mice for disrupted Gm2a gene (*Gm2a*+/-) were mated to generate homozygous mice for Gm2a null mutation (*Gm2a*-/-) (39). Gm2a progeny were obtained in a Mendelian fashion, indicating no embryonic lethality. *Gm2a*-/- mice grew normally and were fertile. Although displaying a normal life span, they showed subtle neurological dysfunction. A total of 24 mice including wild type, *Gm2a*+/- and *Gm2a*-/- were tested beginning at 13 and ending at 33 weeks of age. Overall rotorod performance was significantly impaired in *Gm2a*-/- mice. Passive-avoidance task as a test for learning and memory suggested a possible memory deficit in the *Gm2a*-/- mice. Similar to human patients with G_{M2} activator deficiency, the *Gm2a*-/- mice had normal levels of β-hexosaminidase activity in liver extracts tested using artificial substrates. Sphingolipid analysis at 4 months of age demonstrated an accumulation of G_{M2} ganglioside in the brain of *Gm2a* -/- mice at a comparable level to the *Hexa*-/- mice but less than the *Hexb*-/- mice. In *Hexb*-/- mice, both G_{M2} ganglioside and G_{A2} glycolipid accumulated in the brain while only G_{M2} ganglioside accumulated in the brain of *Hexa*-/- mice at about ¼ level of that noted in the *Hexb*-/- mice. In *Gm2a* -/- mice, in addition to G_{M2} ganglioside, a slight accumulation of G_{A2} was detected. The distribution of storage neurons was very similar to that of *Hexa*-/- with the exception of the cerebellum (Figure 5). In *Gm2a*-/- mice, storage materials were noted in the Purkinje and granular cells and also some cells in the molecular layer in the cerebellum while very little storage was noted in these cells in the cerebellum in *Hexa*-/- mice even at age 18 months. The significant storage in the cerebellum in *Gm2a*-/-, but not in *Hexa*-/- mice, would explain the impaired motor coordination in the former. Little storage was observed in the spinal cord and visceral organs in either knockout mice. The minimal G_{A2} storage in the *Gm2a*-/-mice indicates that the hexosaminidase-mediated degradation of G_{A2} can proceed in the absence of the activator protein (Figure 7). However, ganglioside feeding experiments suggested that the activator protein is likely required for this pathway to proceed optimally. Cerebellar storage in the *Gm2a*-/- but not the *Hexa*-/- could, therefore be due to

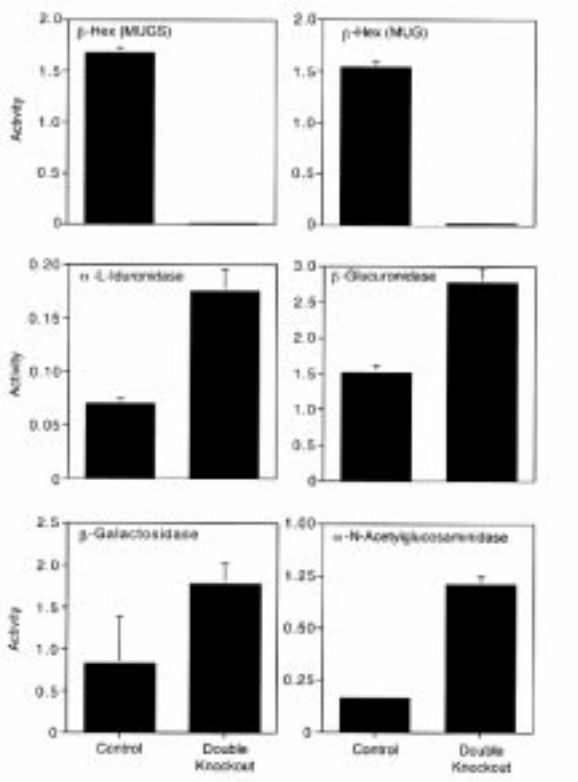

Figure 8. Activities of glycosaminoglycan degrading enzymes are increased in the totally β-hexosaminidase deficient (double knockout) mouse. Liver extracts from double knockout and control mice were assayed using 4-methylumbelliferyl-2-deoxy-β-D-glucopyranoside (MUG) and with the sulfated substrate, 4-methylumbelliferyl-6-sulfo-2-acetamido-2-deoxy-β-D-glucopyranoside (MUGS). MUGS substrate can detect β-hexosaminidase A and S and the MUG substrate can detect β-hexosaminidase A, B and S (see figure 2).
4-methylumbelliferyl-α-L-iduronide was used to detect α-L-iduronidase, 4-methylumbelliferyl-β-D-glucuronide was used to detect β-glucuronidase, 4-methylumbelliferyl-β-D-galactoside was used to detect β-galactosidase and 4-methylumbelliferyl-α-acetylglucosaminidase was used to detect α-N-acetylglucosaminidase. Activity is expressed as nmol substrate cleaved/min/mg protein.

the inability of the activator-independent degradative pathway to handle the level of ganglioside substrate produced in this region of the brain.

Double knockout mice. Mice with both *Hexa* and *Hexb* genes disrupted were produced by interbreeding double heterozygous (*Hexa*+/- *Hexb*+/-) mice or by mating of *Hexa*-/- and *Hexb*+/- mice (60). The "double knockout" (DKO; *Hexa*-/-*Hexb*-/-) mice were totally deficient in all forms of lysosomal β-hexosaminidase including the small amounts of β-hexosaminidase S pre-

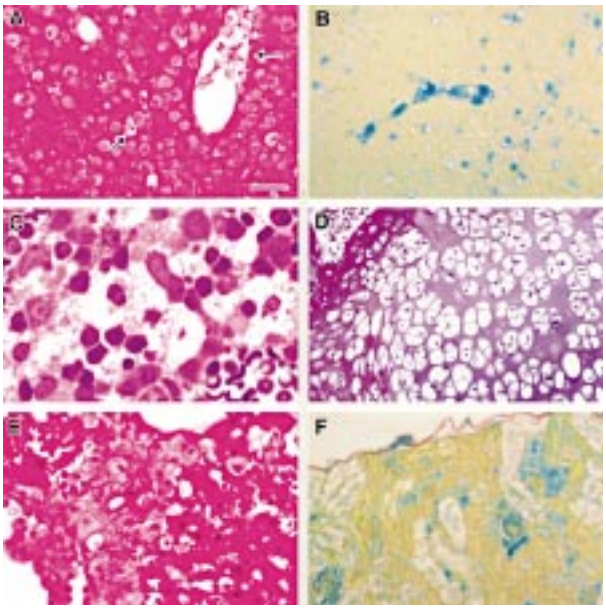

Figure 9. The light micrographs of the cerebral cortex (**A, B**), bone marrow **C.**, cartilage **D.**, liver **E.** and kidney **F.** of the mouse totally deficient with β-hexosaminidase activity (Double knockout mouse). Almost all neurons show perikaryal enlargement with storage material and in addition clear vacuolated non-neuronal cells are scattered or clustered around vessels (arrows)**A.**. These non-neuronal cells stain positive with colloidal iron stain **B.**. The bone marrow contains clear vacuolated cells **C.** and clear vacuoles occupy the entire cytoplasm of chondrocytes **D.**. In the liver **E.**, a large collection of macrophages is conspicuous. All these cells are also stained positive with colloidal iron and alcian blue. Colloidal iron-positive material is clearly noted in the renal tubular epithelium **F.**. (**A, D, E**)-Paraffin sections stained with hematoxylin and eosin; (**B, F**)-Paraffin section stained with colloidal iron stain; **C.**-one micron plastic resin embedded section stained with toluidine blue. Bar for (**A, B, F**), 80μm, for **C.**, 15mm, for (**D, E**), 40mm.

sent in the Sandhoff disease model (*Hexb*-/-) mice (Figure 2). Total deficiency of lysosomal β-hexosaminidase is not known in humans at this time. Unexpectedly these mice showed clinical, pathologic and biochemical features of severe mucopolysaccharidosis. At birth these mice were indistinguishable from their littermates but by 4-5 weeks, DKO mice could be distinguished by their smaller size and physical dysmorphia. Their heads were shorter and the snouts broader. Their feet were thick and broad with flexion contracture of the digits. Corneal opacities were present. Occasional seizure-like activity and unresponsiveness to sharp noise suggesting deafness were also noted. Radiographic study showed kyphosis, an abnormally shaped rib cage and short and thickened long-bones. Their life span was 1 to 4 months. As expected none of the β-hexosaminidase isozymes were detectable in liver extracts (Figure2). Sphingolipid analysis of the brain showed massive accumulation of G_{M2} ganglioside and its asialo derivative G_{A2} to the degree comparable to the level of *Hexb*-/- mouse brain. Feeding experiments with embryonic fibroblasts from DKO mice demonstrated a block in the ganglioside degradation pathway comparable to that seen in the *Hexb*-/- mice. The urine of these mice contained large amounts of glycosaminoglycans consisting of N-acetylgalactosamine and iduronic acid consistent with dermatan sulphate, and galactose suggestive of the presence of keratan sulfate. However, the activity of enzymes involved in classical degradation pathway of glycosaminoglycans such as α-N-acetylglucosaminidase, α-L-iduronidase, β-glucuronidase and β-galactosidase were higher than wild type control mice (Figure 8). A kinetic study with embryonic fibroblasts showed linear accumulation of glycosaminoglycans in the DKO fibroblasts, a pattern similar to that seen in cells of mucopolysaccharidoses patients where synthesis proceeds in the absence of degradation.

Pathology of the DKO mice was closely similar to mucopolysaccharidoses (73). The pathological features of known mucopolysaccharidoses are very similar to each other. They consist of storage of glycosaminoglycans in tissue macrophages and in certain tissue elements such as chondrocytes, splenic sinusoidal cells etc and various degree of neuronal storage(see description in mucopolysaccharidoses models below). In DKO mice, macrophages containing PAS, alcian blue and colloidal iron stained materials (consistent with glycosaminoglycans) were noted in the bone marrow (Fig 9C), dermal tissue, adipose tissue and connective tissues around visceral organs. These cells were also in the myocardium, heart valves, lung, liver (Fig 9E), spleen and kidney. The renal tubular epithelium (Fig 9F) and smooth muscle cells in the media of the aorta and arteries as well as chondrocytes (Fig 9D) and osteocytes contained colloidal iron positively stained materials. In the central nervous system, neuronal storage (Fig 9A), similar in extent to that seen in *Hexb*-/- mice was noted throughout. In addition, there were numerous small cells (tentatively identified as macrophages) with distended cytoplasm containing colloidal iron and alcian blue positive materials in the brain, leptomeninges and choroid plexus stroma. Some were located closely juxtaposed to blood vessels (Figure 9B). These cells stained strongly positive with lectin RCA-1. The white matter was diffusely hypomyelinated with increased numbers of GFAP immunoreactive astrocytes and RCA-1 stained microglia/macrophages. In the white matter nerve fiber

tracts, many axonal spheroids and scattered myelin figures suggestive of myelin degeneration were recognized at the terminal stage of disease. In the PNS, neuronal storage was noted in the trigeminal and dorsal root ganglia, neurons in the myenteric plexus and visceral autonomic ganglia. Macrophages similar to those found in the brain were also very conspicuous in the peripheral nerves, although nerve fibers appeared well preserved. These morphological features together with biochemical data indicate β-hexosaminidase is a crucial enzyme in the degradation of glycosaminoglycans. Although a few colloidal iron containing cells were found in the brain of *Hexb*-/- mice, lack of significant glycosaminoglycan storage in these mice and in human cases of Tay-Sachs and Sandhoff disease is due to functional redundancy in the β-hexosaminidase system. Apparently the presence of minor isozyme S in Sandhoff disease is sufficient to prevent massive accumulation of glycosaminoglycans. These completely hexosaminidase-deficient mice are not a model of a known lysosomal storage disease in humans but are a valuable tool for studying the role of the β-hexosaminidase in the degradation of glycosaminoglycans and in understanding the pathological consequences of excessive accumulation of glycosaminoglycans.

G_{M1} gangliosidosis

G_{M1} gangliosidosis is a progressive neurological disease caused by a genetic deficiency of lysosomal acid β-galactosidase. Three clinical types, infantile, juvenile and adult types, are known. The clinical course is most rapidly progressive in the infantile type and is usually associated with storage in the visceral organs and with mucopolysaccharidosis like dysmorphic features. Patients with the infantile type of G_{M1} gangliosidosis usually succumb to the disease within a few years. In later-onset types, the clinical course is more prolonged and visceral involvement is less common. The adult type is the most chronic form and often manifests as a movement disorder. Radiological evidence of bony abnormalities are frequently recognized. Morquio B disease is also caused by β-galactosidase deficiency and occurs at various ages. Unlike the other types mentioned, this type shows almost no neurological symptoms; the main clinical symptoms are related to severe bony deformities. Patients with intermediate clinical form have also been reported (74, 76). The infantile type shows diffuse neuronal storage of G_{M1} ganglioside and, to a lesser extent, its asialo derivative G_{A1}. Oligosaccharides derived from keratan sulfate and glycopeptides are stored primarily in the visceral organs and excreted into the urine (70). In the chronic adult type, neuronal storage tends to be more localized in the basal ganglia and cerebellum (71). The human acid β-galactosidase cDNA and gene has been cloned and characterized and many disease-causing mutations have been identified (8, 11, 48, 71, 75).

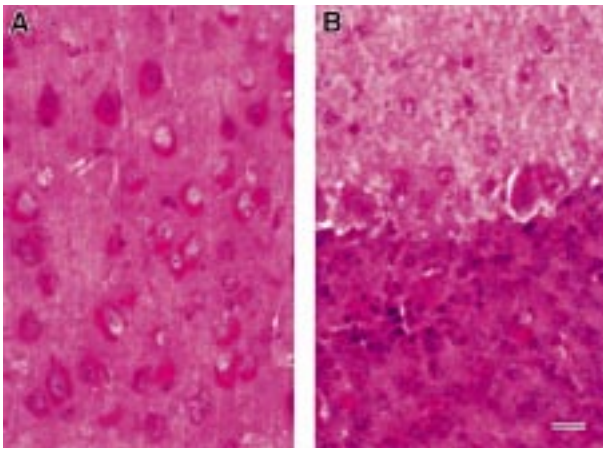

Figure 10. Cerebral cortex **A.** and cerebellum **B.** of a β-gal-/- mouse at age 3 weeks showing extensive storage in practically all neurons. Frozen sections stained with PAS. Bar 20μm

Mouse model. Recently a mouse model lacking a functional β-galactosidase gene (β-gal-/-) has been generated by homologous recombination and embryonic stem cell technology by two groups of investigators(24, 41). The β-gal gene consists of 16 exons and was inactivated by introducing Neo cassette into the middle of exon 6 (24) or exon 15 (41). The genotype analysis of 117 newborn animals (from 15 litters of heterozygous crossing) in our group indicated a Mendelian inheritance ratio among β-gal-/-, +/- and +/+ mice. Thus, neither embryonic nor fetal lethality occurred. The β-gal -/- mice are fertile and appeared phenotypically normal until about 4-5 months of age when generalized tremor, ataxia and abnormal gait became apparent. No β-gal mRNA was detected by northern blot analysis of kidney, brain and liver. β-galactosidase activity in the kidney, brain, liver and spleen was markedly decreased (ranging from 1% in the spleen to 4% in the brain) compared with wild type littermates. By thin layer chromatography, markedly increased G_{M1} ganglioside and its asialo derivative G_{A1} was noted in the brains of β-gal -/- mice. In the brain of humans with infantile G_{M1} gangliosidosis, G_{M1} ganglioside markedly accumulates with a far lesser degree of G_{A1} accumulation. Thus, marked accumulation of G_{A1} in this mouse model may suggest that the murine sialidase is more active toward G_{M1} ganglioside than the

corresponding human enzyme analogous to G_{M2} degradation in the mouse (Figure 7). In β-gal-/- mice, the total amounts of brain ganglioside sialic acid and G_{M1} ganglioside increased dramatically during the progression of the disease from 3 weeks to 3.5 months of age. On histological preparation, neuronal storage was already widespread as early as 3 weeks of age (Fig 10). By 5 weeks, PAS stained storage materials were seen in almost all neurons in the cerebrum, cerebellum, brainstem and spinal cord and spinal dorsal root ganglia. Diffuse neuronal storage in these mice was very similar to the pattern of neuronal storage noted in the infantile G_{M1} gangliosidosis. Ultrastructural features of neuronal storage materials (inclusions) were also similar to those of infantile G_{M1} gangliosidosis. Unlike the human disease, β-gal-/- mice show no hepatosplenomegaly and no storage materials were detected in visceral organs even at 3.5 months. Biochemical analysis showed only minimal storage of oligosaccharide in the liver and a low level of abnormal urinary oligosaccharides. The β-gal-/- mice reported by Matsuda and co-workers (41) also were apparently healthy for the first 4 months. Subsequently, horizontal movement became slower and rearing or vertical climbing became less frequent. Definite gait disturbance was noted by 6-8 months of age. They describe that β-gal-/- mice showed unusual postures with all four limbs flexed when hung vertically with the tail held upward. Spastic diplegia progressed and the mice died of extreme emaciation at 7-10 months of age because of difficulty in feeding. They described ballooning of neurons in various areas of the central nervous system and 20-30 fold increase of G_{M1} ganglioside in the brain of these mice. β-galactosidase activity of β-gal-/- fibroblasts was reported to be 0-1% of control value (41). Thus, both of these mouse models are similar to the infantile type of G_{M1} gangliosidosis as far as the CNS involvement is concerned. Minimal involvement of visceral organs in the mouse model may suggest differences in the metabolic pathway in these organs between humans and mice.

Galactosialidosis

Galactosialidosis is an autosomal recessive lysosomal storage disease caused by mutations of the gene encording a 32/20-kDa protective dimeric protein with cathepsin A-like activity (protective protein/cathepsin A; PPCA). This protein forms a complex with the two lysosomal enzymes, β-galactosidase and sialidase and thus deficiency of PPCA secondarily causes a combined deficiency of β-galactosidase and sialidase (N-acetyl-α-neuraminidase) (14, 88). Three phenotypic subtypes, early infantile, late infantile and juvenile/adult types, are known. The early infantile type is associated with fetal hydrops, edema, ascites, visceromegaly, skeletal dysplasia and death within the first year of age. The late infantile type is characterized by hepatosplenomegaly, growth retardation, cardiac involvement, and absence of relevant neurologic signs. The juvenile/adult cases appear to be the most common phenotype, in particular in Japan. They manifest slowly progressive neurological deterioration with mental retardation,; myoclonus, ataxia, macular cherry-red spot, angiokeratoma, and facial and/or skeletal dysmorphia are often associated features (14). Malfunction of the protective protein leads to intralysosomal proteolysis of the enzymes, that result in an accumulation of sialyloligosaccharides in cellular lysosomes and excessive excretion of sialyloligosaccharides in urine, a diagnostic feature of this disease. Multiple cytoplasmic vacuoles were found in varieties of cell types in the central, peripheral and autonomic nervous system, retina, liver, kidney, skin and leukocytes (49, 93) and membranous lamellar inclusions have been described in neurons (49, 54, 93).

Mouse model. With disruption of the mouse PPCA gene by inserting the *hygro* cassette into exon 2, a murine model for galactosialidosis has been generated (97). These mice carrying a null mutation at the PPCA locus (PPCA-/-) were viable and fertile. They were normal during early development except for an apparent flattening of the face. However, they usually weighed less (25-40% less) than PPCA+/- or +/+ mice. With age, progressive and diffuse cutaneous edema accompanied by ataxia and tremor became apparent. By 10 months of age, the characteristic broad face, rough coat, and extensive swelling of subcutaneous tissues, limbs and eyelids were obvious. These features closely resemble galactosialidosis in human patients. PPCA-/- mice usually die at 12 months of age. Cathepsin A activity was absent or markedly reduced in PPCA-/- mice (non-detectable in bone marrow to 8% of normal in the liver). Urinary sialyloligosaccharides increased progressively with time, reaching levels 25 times higher than controls at the age of 6-8 months. Activity of neuraminidase was severely reduced, especially in fibroblasts and kidney. However β-galactosidase levels varied considerably. In human patients, PPCA deficiency results in the combined deficiency of both neuraminidase and β-galactosidase but apparently this was not the case in this murine model, suggesting that murine β-galactosidase may be less dependent for its stability and activity on complex for-

mation with PPCA than murine neuraminidase. As noted in infantile cases of galactosialidosis, hepatosplenomegaly was present in PPCA-/- mice that died spontaneously at 3 weeks of age. Vacuoles were identified in 30% of lymphocytes in the peripheral blood. Macrophages with clear vacuoles were seen in the dermal tissue and connective tissues around visceral organs. Vacuolation was noted in the renal tubular epithelium and was most evident in the proximal tubules in early stage. In the later stage, abundant vacuolation was evident in the parietal and visceral epithelium, endothelium and mesangial cells. Vacuolation was also noted in the Kupffer cells, hepatocytes, splenic macrophages (Figure 11D). These vacuoles contained PAS positive materials. In the brain, vacuolated cells similar to the macrophages in the visceral organs were found often at perineuronal or perivascular locations. The choroid plexus epithelial cells were conspicuously vacuolated with storage materials (Figure 11B). There was a significant regional variation in neuronal storage. For example, neuronal storage was more pronounced in the entorhinal cortex (Figure 11A) and hippocampus than somatosensory cortex. Neuronal storage was also noted in the trigeminal and spinal dorsal root ganglia (Figure11C). In the peripheral nerve, many vacuolated cells were scattered among well myelinated fibers. Thus pathological features of PPCA-/- mice closely resemble the most severe forms of galactosialidosis in humans, although the mouse model showed prolonged survival.

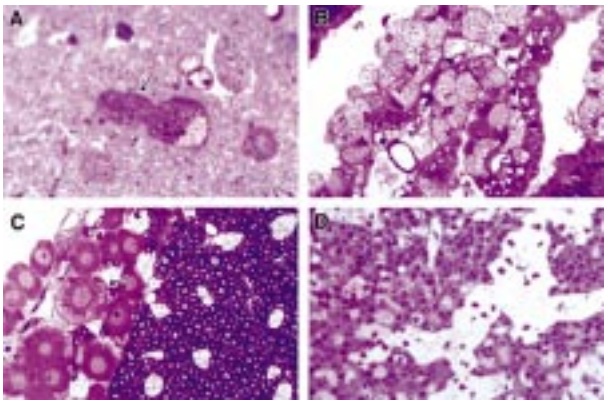

Figure 11. Light micrographs of the entorhinal cortex **A.**, choroid plexus **B.**, trigeminal ganglion **C.** and spleen **D.** of a PPCA-/- mouse. The neuronal perikaryon is packed with granular inclusions with possible formation of a meganeurite (an arrow) in **A.**. The epithelial cells in the choroid plexus are finely vacuolated **B.**. Storage material is noted in some ganglion cells (arrow) in the trigeminal ganglia. The trigeminal nerve fibers appear intact despite presence of foamy vacuolated cells **C.**. In the spleen foamy macrophages with clear cytoplasm are very conspicuous **D.**. All are one micron plastic resin embedded sections stained with toluidine blue. Bar for **A.**, 12μm, for (**B, C, D**), 30μm

Niemann-Pick disease, type A and B

Niemann-Pick disease (NPD) is an autosomal recessive neurodegenerative disease caused by deficient activity of the lysosomal enzyme acid sphingomyelinase. Two clinical types, A and B are known. Type A patients have severe neurovisceral storage and usually die by three years of age. Type B patients have little or no neurological manifestation and often survive until adulthood. The mechanism for such a phenotypic difference is not well understood. The locus for the acid sphingomyelinase gene is on chromosome 11 and several different mutations, mostly point mutations, that caused type A or type B of NPD have been identified. Sphingomyelin and cholesterol accumulate within the cells of the reticuloendothelial system causing massive hepatosplenomegaly. In addition diffuse neuronal storage was conspicuous a neuropathological finding in the type A patients (64, 83).

Mouse model. Recently two groups of investigators generated murine models of NPD by disrupting the acid sphingomyelinase gene with insertion of Neo cassette into exon 2 (33) or 3 (52). The acid sphingomyelinase null mutant (asmase-/-) mice generated by Otterback and Stoffel (52) were normal until 8-10 weeks of age when a fine tremor of the entire body and a severe intention tremor developed. Their gait became increasingly ataxic and displayed tottering with zigzag movement characteristic of cerebellar dysfunction. Around 60 days of age hepatosplenomegaly became apparent and the asmase-/- mice died around 4 months of age after a period of severe dyspnea. In the total protein extracts of liver, spleen and brain of asmase-/- mice, no acid sphingomyelinase activity was measurable. Northern blot analysis of total RNA of liver, spleen and brain of asmase-/- mice revealed no acid sphingomyelinase specific transcript. Residual neutral sphingomyelinase activity in the brain, however, was similar to that of wild type mice. Accumulation of sphinomyelin was detected in the liver and spleen and to a lesser extent in the brain. The liver and spleen of asmase-/- mice increased about 1.5 and 2 times in weight, respectively in the terminal stage. Massive accumulation of the lipid was histologically evident in Kupffer cells and other tissue macrophages in the bone marrow, spleen and lung. The brain weight and volume appeared similar to that of age matched controls. Neurons in the central nervous system were frequently swollen with pale vacuolation. The cerebral cortical structures were slightly disturbed. The most striking feature in the brain of asmase-/-mice was

a loss of Purkinje cells in the cerebellum which occurred within 60-90 days after birth and molecular cell layer became very narrow in the final stage of the disease (at days 210 and 225) (37). Thus, this murine model is phenotypically as well as pathologically closely similar to Niemann-Pick disease type A in humans.

The acid sphingomyelinase knockout (ASMKO) mice generated by Horinouchi and co-workers (33) showed ataxia and mild tremor around 8 weeks and feeding difficulty but survived longer and was fertile. Death in these mice occurred much later than the previous mice at between 6 and 8 months of age. Unlike the previous mice that showed no significant brain atrophy, the brain of ASMKO mice were atrophic and less than half the weight and volume of control mice. A remarkable loss of Purkinje cells and general atrophy of the cerebellum and midbrain was evident. Hepatosplenomegaly, that was a striking feature in amass-/- mice generated by Otterback and Stoffel, was not evident in these mice , although lipid laden foam cells (NPD cells) were found in most major organs, particularly in bone marrow and spleen. Multilamellar inclusions were demonstrated in the neurons in both mutant mice at the ultrastructural level (33, 37). Thus ASMKO mice generated by Horinouchi and co-workers showed longer survival with severe cerebral atrophy but without hepatosplenomegaly. Reason for such phenotypic difference and extent of pathology between these two acid sphingomyelinase deficent mice is not clear.

Fabry disease

Fabry disease is an X-linked metabolic disorder of glycolipid caused by a deficiency of the lysosomal enzyme α-galactosidase A (α-Gal A) (15). Neutral glycosphingolipids with terminal α-linked galactosyl moieties- predominantly ceramidetrihexoside [globotriaosylceramide] and to a lesser extent galabiosylceramide Galα1-4-Gal b1-1Cer) accumulate in the endothelial, perithelial and smooth muscle cells of blood vessels and many other cell types in the liver, heart, spleen, kidney and in plasma of the patients. Classical clinical manifestations include pain and paresthesia in the extremities, angiokeratoma in the skin and mucous membranes, and hypohidrosis during childhood or adolescence. Corneal and lenticular opacities may be present. With increasing age, severe renal failure caused by progressive glycosphingolipid accumulation results in hypertension and uremia. The hemizygous male patients usually die of renal, cardiac or cerebrovascular disease. Late onset milder disease with primary cardiac involvement ("cardiac variant") is known. Heterozygous females may have an attenuated form of the disease, although they are usually asymptomatic. The gene encoding α-galactosidase is localized to Xq22. The molecular lesions causing this disease are heterogenous and partial gene rearrangements, splice-junction defects and point mutations have been identified. Characteristic pathology is wide spread tissue deposits of crystalline glycosphingolipids, which show birefringenece with characteristic "Maltese crosses" under polarizing microscopy. The glycosphingolipid is deposited in all areas of the body predominantly vascular endothelial, perithelial and smooth muscle cells, epithelial cells of the cornea, glomeruli and tubules of the kidney, in cardiac muscle fibers and ganglion cells in the autonomic nervous system. The lipid deposits were also reported in neurons in certain region in the brain and spinal cord (16, 58, 69).

Mouse model. The mouse model of Fabry disease generated by targeted gene disruption has been reported recently (51). Heterozygous female mice α-Gal A (+/-) were mated with α-Gal A (+/0) male mice. Hemizygous male mice, α-Gal A (-/0), were born in the expected ratio. α-Gal A activity was undetectable in liver homogenates from α-Gal A(-/0) mice. These mutant mice were clinically normal at 10-14 weeks of age. No obvious histological lesions were detected in the kidney, liver, heart, spleen, lungs and brain on routine sections stained with hematoxylin and eosin. However, lipid inclusions consisting of concentric lamellar structures were observed at the ultrastructural level in the renal tubular epithelium. They appeared similar to those seen in patients with Fabry disease. With fluorescent-labeled Griffonia (Bandeiraea) simplicifolia lectin which selectively binds to α-D-galactosyl residues, significant accumulation of compounds containing α-D-galactosyl residues was demonstrated in the kidney of 10 week old mutant mice. Cutaneous fibroblasts from α-Gal (-/0) mouse embryos also displayed significant accumulation of α-Gal A substrates. Significant accumulation of ceramidetrihexoside (CTH) was observed in the liver and kidney by HPTLC (High Pressure Thin Layer Chromatography) . Thus, the authors anticipate that as the α-Gal A deficient mice age, CHT will continue to accumulate and that their phenotype will more closely resemble that of Fabry patients.

Metachromatic leukodystrophy (MLD)

Metachromatic leukodystrophy (MLD) is an autosomal recessive lysosomal storage disease caused by a deficiency of arylsulfatase A (ASA) (36). Deficiency of ASA results in an accumulation of the substrate, sul-

fatide, in various organs including the brain. Sulfatide is a major myelin lipid and perturbed sulfatide metabolism causes diffuse demyelination of the CNS white matter and peripheral nerves. Late infantile, juvenile and adult types are known clinically. The late infantile MLD is the most common type with rapidly progressive neurological symptoms such as psychomotor deterioration with blindness, seizures, quadriparesis and peripheral neuropathy, usually manifesting in the second year of life. Patients with this type usually die within a few years. Juvenile and adult types were more slowly progressive and neurological symptoms were recognized between age 4 and 12 years or between mid-teens and the seventh decade respectively. Behavioral disturbance or dementia are the major presenting signs and often with progressive peripheral neuropathy. In all types, ASA is markedly deficient in tissues. The ASA gene is located near the end of the long arm of chromosome 22 and more than 30 disease-related mutations have been identified (20). The pathology of MLD in the nervous system is primarily a diffuse demyelination in association with deposits of metachromatic materials (sulfatide) in kidney, gallbladder, liver, pancreas and various other visceral organs and in the brain (90) In the brain metachromatic material accumulates in glial cells and neurons in certain regions such as dentate nucleus of the cerebellum, some brain stem nuclei, spinal anterior horn etc (55). The storage materials stain brown in frozen sections, when treated with acidic cresyl violet (84). Prismatic and tuffstone inclusions were characteristic ultrastructural features of these metachromatic deposits (22).

Mouse model. The mouse model of MLD was generated recently by targeted disruption of the ASA gene (29). ASA mRNA was completely deficient in the ASA-/- mice. With a sulfatide loading assay, no turnover of sulfatide was detected in fibroblasts and oligodendrocytes from ASA-/- mice, indicating a complete absence of ASA activity. Thus, biochemically the ASA-/- mice resemble the severe late infantile MLD. However, clinically ASA-/- mice showed a much milder phenotype. In ASA-/- mice at 12-14 months of age, statistically significant but subtle abnormalities were detected in neuromotor function and behavior when they were evaluated by walking pattern, rotorod test and Morris water maze. The authors suggested that the impairment of neuromotor coordination in ASA-/- mice resembles early stages of human disease. The most notable neurological sign in ASA-/- mice was totally absent auditory brainstem evoked potentials. In the second year of life, ASA-/- mice developed a low frequency tremor of the head. Sulfatide storage was noted histologically in the kidneys, gall bladder and bile duct of mice at ages 6-11 months. However, the storage was not as widespread as that seen in human patients and no evidence of storage was noted in hepatocytes, adrenal glands, skeletal muscle etc. In the brain of 11 month-old ASA-/- mice storage of metachromatic material (sulfatide) was noted in the white matter (corpus callosum, hippocampal fimbria, internal capsule and optic nerve) but demyelination was not apparent. An ultrastructural study demonstrated lamellar deposit, herringbone patterns and tuffstone like materials, similar to those found in human MLD, in astrocytes, oligodendrocytes, microglia and Schwann cells. Myelin sheaths had a normal ultrastructure. However, there was a statistically significant reduction of axon cross-sectional area of myelinated fibers in the corpus callosum and optic nerve of ASA-/- mice. Sulfatide accumulation increased with age as more sulfatide deposits were noted in 2 year-old than 1 year-old mice. Activation of microglia became conspicuous with age as well, although astrogliosis was present even at 1 year of age. Neuronal storage was observed in several nuclei of the brainstem, diencephalon, spinal cord and cerebellum. Neuronal damage was dramatic in the inner ear of ASA-/- mice. The number of acoustic ganglion cells and myelinated nerve fibers were greatly reduced. The Schwann cells in the acoustic and vestibular ganglion showed marked sulfatide storage. Storage was also evident in the Schwann cells in the peripheral nerve but demyelination was not present. Thus, basic pattern of pathological process in ASA-/- mice is highly reminiscent to human MLD pathology but the process is milder.

Total sphingolipid activator protein (prosaposin) deficiency

Sphingolipid activator proteins (SAPs) are small nonenzymatic lysosomal glycoproteins which function as essential cofactors for physiological degradation of sphingolipids with relatively short hydrophilic head groups (62). Two genes encode all established and putative SAPs known so far. One is the G_{M2} activator protein localized on chromosome 5 that stimulates degradation of G_{M2} ganglioside and asialo G_{M2} ganglioside (G_{A2}) (10). The other gene is on chromosome 10 coding for the SAP precursor, which is processed to the four activator proteins, SAP-A, SAP-B, SAP-C and SAP-D. These SAPs are homologous to each other and are encoded tandemly by a single gene , a sap precursor gene. Genetic deficiencies of SAP-B (sulfatide activator) (44) or SAP-C (glucosylceramide activator) (30) in man result in disorders mimicking metachromatic leukodystrophy and

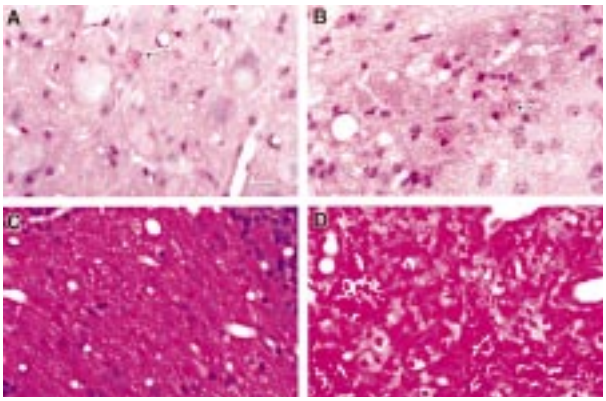

Figure 12. Light micrographs of the cerebral cortex **A.**, white matter **B.**, cerebellar white matter **C.** and spleen **D.** of a SAP-/- mouse. The perikarya of cerebral cortical neurons are swollen with storage material **A.**. Many PAS positive macrophages (arrows) are present in the white matter **B.** and to far lesser extent in the cortex **A.**. Deeply eosinophilic axonal spheroids are numerous in the cerebellar white matter **C.**. Macrophages are conspicuous in the spleen **D.**. (**A, B**)-frozen section stained with PAS and hematoxylin; **C.**-Paraffin section stained with solochrome and eosin; **D.** paraffin section stained with hematoxylin and eosin. Bar 10μm.

Gaucher disease, respectively. In 1989, Harzer and coworkers reported two sibs in a consanguineous family, affected by a rapidly fatal disorder(25). None of the SAPs were detected in the tissue from these sibs (9) and they were later found to be homoallelic for a mutation in the initiation codon of the SAP gene (63). The clinical phenotype resembled severe infantile type of Gaucher disease (type II). Shortly after birth, the patient showed hyperkinetic or cloniform motor abnormalities and generalized clonic seizures. The patient had fasciculation of tongue and periauricular muscle, spontaneous Babinski signs and an exaggerated Moro reflex. Massive hepatosplenomegaly was present and storage macrophages resembling Gaucher cells were observed in a bone marrow smear at the age of 5 weeks. The enzyme studies with leukocytes and cultured fibroblasts showed a profound deficiency of β-galactosylceramidase and partial deficiency of β-glucosylceramidase activity. The ultrastructure of liver, nerve and skin biopsies revealed the presence of vesicular inclusions and membranous bodies suggestive of lysosomal storage disease. An in situ test with cultured fibroblasts demonstrated a defect in ceramide catabolism similar to Farber disease. Neuroimaging revealed an atrophic brain with hydrocephalus. Postmortem examination was not performed, however. The second patient, an aborted female sib of the first patient showed similar defect in the ceramide catabolism and had contracted hand joints consistent with a Farber-like disease. The SAP precursor and mature SAPs were completely absent in this fetus who had generalized accumulation of multiple sphingolipids (ceramide, glucosylceramide, galactosylceramide, sulfatide, lactosylceramide, digalactosylceramide, ganglioside G_{M1} etc) with exception of sphingomyelin in the brain and systemic organs.

Mouse model. The SAP gene was disrupted by insertion of the neomycin-resistant gene within exon 3 and SAP-/- mice were generated (19). SAP mRNA was completely absent in the tissue of SAP-/- mice. Of the first 126 offspring from heterozygous mating, 36 (26%) wild type, 68 (55%) heterozygotes and 16 (13%) homozygotes were obtained. Five of the total 9 mice that died within a day or two of birth were SAP-/- mice. These results suggested that a disproportionate percentage of SAP-/- mice die in utero or the perinatal period. Those SAP-/- mice that survived the neonatal period were apparently healthy until about 18-20 days, although they were slightly smaller in size. Tremulousness of the head and mild weakness/ataxia of the initial symptoms manifesting around 20 days of age. These symptoms progress rapidly and SAP-/- usually die around 35 days of age in an emaciated general condition. The pathology of SAP-/- mice was that of combined neuronal storage and leukodystrophy. The brain and visceral organs were of normal size except for the kidneys which were smaller than control. There was extensive neuronal storage throughout the cerebrum (Figure 12A) cerebellum, brainstem, spinal cord and retinal ganglion cells. The storage materials stained brilliantly red with PAS on frozen sections. Many axonal spheroids (Figure 12C) and macrophages/microglia containing storage materials were also conspicuous (Fig 12B). The white matter was hypomyelinated but myelin ovoids suggestive of myelin degeneration was also noted in the corpus callosum, internal capsule and spinal white matter. Similar changes of myelin were noted in the spinal roots, trigeminal and sciatic nerves. No metachromatic or sudanophilic materials were found in the frozen section of the cerebrum. In the liver, clusters of histiocytes with abundant eosinophilic cytoplasm were noted in the hepatic sinusoids. Similar cells were also noted in the spleen and lymph nodes (Figure 12D). No significant abnormalities were detected in the kidney despite smaller size. The inclusions in neurons were pleomorphic at the ultrastructural level; some consisted of concentric or short lamellar structures combined with electron dense granular structure and others are electron dense granular structures surrounded by a sin-

gle membrane. Small clusters of electron dense granular material or small concentric lamellar structures were scattered within the cytoplasm of some neurons. These inclusions resembled those of cultured skin fibroblasts from the patient with total SAP deficiency. The inclusions within the cells in the hepatic sinusoids also consisted of membranous and vesicular structures and were more complex than neuronal inclusions (53). Biochemically the most conspicuous specific abnormality was a major accumulation of lactosylceramide which appeared to account for the strong PAS staining on frozen section. The total ganglioside sialic acid was increased significantly with a large relative increase in the monosialoganglioside G_{M1}, G_{M2} and G_{M3}. Similar to the brain, lactosylceramide was conspicuously increased in the liver and kidney. Additionally, ceramide, glucosylceramide, globotriaosyl-ceramide and globoside were all significantly increased in the liver. Galactosylceramide and sulfatide accumulated in the kidney. Thus, accumulation of varieties of sphingolipids noted in patients with SAP deficiency was also noted in in SAP-/- mice. As noted in human patients, activity of glucosylceramidase and galactosylceramidase were decreased in SAP-/- mice. Therefore, SAP-/- mice mimic biochemical changes of human patients with total SAP deficiency. Neuropathology could not be compared, however, since postmortem investigation was not carried out on the original patient with SAP deficiency.

Mucopolysaccharidoses

The mucopolysaccharidoses (MPS) are a group of lysosomal storage disorders caused by deficiency of enzymes catalyzing the stepwise degradation of glycosaminoglycans (mucopolysaccharides). Lysosomal accumulation of glycosaminoglycan molecules results in damage of targeted cells and eventual organ dysfunction. Glycosaminoglycans fragments generated by alternative degradation pathways are excreted in urine. There are 10 known enzyme deficiencies that give rise to distinct types of MPS. All types share variable degrees of common clinical features of MPS that include abnormal faces, dysostosis multiplex and organomegaly. Hearing, vision, cardiovascular function and joint mobility may be affected. Profound mental retardation can be found in some types (MPS I , II, III) while in others (MPS IV) bony abnormalities may be a major clinical problem (47). There are several naturally occurring animal models of MPS ; canine and feline MPS I (28, 66), caprine MPS IIID (81), feline and rat MPSVI (17, 34, 96), canine and murine MPSVII (7, 27).

Mouse models. Recently murine models of MPS I and VI have been generated by targeted gene disruption.

Mucopolysaccharidosis type I (MSP I) mouse. MPS I, considered to be the prototype of MPS, is caused by a deficiency of α-L-iduronidase and represents the most common subtype. The spectrum of clinical phenotypes in MPS I ranges from severe mental retardation with hepatosplenomegaly, dysostosis multiplex, corneal clouding, cardiac involvement and death in early childhood to milder symptoms consisting of corneal clouding, hearing loss and mild visceral involvement with normal intelligence and life span. Hurler syndrome (MPS IH) represents the most common and severe form and Scheie syndrome (MSP IS) represents the milder form. There is a good genotype/phenotype correlation in human cases of MPS I (65). The targeted disruption of murine *Idua* gene resulted in the lack of expression of *Idua* mRNA and mice totally deficient in activity of α-L-iduronidase (*Idua*-/- mice) were generated (12). The enzyme activity was not detectable in homogenates of liver, kidney, brain and tail clippings of these mice. Urinary glycosaminoglycan secretion was markedly increased (2 fold at 4 weeks and 5 fold at 15 weeks old mice). *Idua*-/- mice were apparently normal clinically during the first 2-3 post-natal weeks. At 4 weeks of age, however, characteristic facial abnormalities of MPS I (broadness of the face with a loss of the fine tapered snout) and broadened and thickened digits and palmar region of the paws were discernible. Prominent features of dysostosis multiplex were noted radiographically at 15 weeks of age. However, weight gain of *Idua*-/- and control mice were similar without any increase in mortality in the former during the first 20 weeks of life, and *Idua*-/- mice were fertile. No hepatosplenomegaly was detected. The pathology was that of diffuse lysosomal storage disease largely involving cells of the reticuloendothelial system such as Kupffer cells, splenic sinusoidal lining cells, pulmonary macrophages, and chondrocytes and glial cells. Cytoplasmic vacuolation indicative of lysosomal storage was noted in these cells as early as 4 weeks. Cytoplasmic vacuolation was noted in neurons at 8 weeks but not at 4 weeks. Thus, biochemically and pathologically *Idua*-/- mice closely resemble severe MPS I in humans.

Mucopolysaccharidosis VI mice. Mucopolysaccharidosis VI (MPS VI) or Maroteaux-Lamy syndrome is an autosomal recessive lysosomal storage disease caused by a deficiency of lysosomal enzyme arylsulfatase B

(ASB; N-acetylgalactosamine-4-sulfatase). The patients show dysmorphic skeletal abnormalities (dysostosis multiplex with macrocephaly, deformities of the chest and vertebral bodies, pelvic bones and dysplasia of long bones) similar to MPS I, but mental development is normal. Corneal clouding, hernia, thickened skin, hepatosplenomegaly, cardiac involvement with valvular dysfunction are common. Multiple mutations in the arylsulfatase B gene have been detected in MPS VI patients. The arylsulfatase B deficient (Asl-s-/-) mice were generated by disruption of ASB structural gene (Asl-s) (18). In the tissue homogenates of these mice, no arylsulfatase B activity was detected. At birth and first postnatal week, Asl-s-/- mice could not be distinguished from littermate controls. Facial dysmorphia, shortened limbs and coarse paws became apparent around 4 weeks of age. Symptoms progressed and at age 9-12 months, the body weight of Asl-s-/- mice were about 15% less than that of controls. Urinary excretion of glycosaminoglycans was increased. Coarse granular inclusions equivalent to the Alder-Reilly bodies in human MPSVI were observed in almost all polymorphnuclear leukocytes and about 50% of the lymphocytes. The Asl-s-/- mice were fertile, and no increase in mortality was noted up to an age of 15 months. In addition to bony abnormalities, a striking radiographic abnormality in Asl-s-/- mice was persisting growth plates at long bones and tail vertebrae at 4 or even 8 months of age when growth plates completely disappeared in control mice. Abnormalities in bone and cartilage with ballooned vacuolated chondrocytes were noted in the vertebrae and skull of the newborn Asl-s-/- mice. Accumulation of glycosaminoglycans was widespread in interstitial fibroblast-like cells and macrophages in all tissues investigated histologically. Parenchymal cells only rarely contained storage material. With exception of leptomeninges and choroid plexus stroma in older mice, no storage of glycosaminoglycans was observed in the brain of Als-s-/- mice. All these pathological features observed in this mouse model are comparable with that of human patients.

Aspartylglucosaminuria

Aspartylglucosaminuria is the most common disorder of glycoprotein degradation in Finland. Only rare isolated cases are reported elsewhere. It is caused by a deficiency of lysosomal enzyme glycosylasparginase (Aga) resulting in tissue accumulation of aspartylglucosamine. The clinical course is that of slowly progressive psychomoter retardation, and patients usually die in the third to fifth decade with pulmonary infection. The patients are relatively healthy for the first year of life except for recurrent infection, diarrhea and hernia. In later childhood, head circumference and stature are decreased and hepatomegaly may be present. With age, sagging skin folds and coarsening of the faces progressively become obvious. Mental retardation is detected between the ages of 6 and 15 years. Behavioral abnormalities and skeletal dysplasia have been reported. Only very limited reports on the pathology are available. The most notable finding is vacuolated cytoplasm of various cells with variable PAS staining (80).

Mouse model. Through targeted disruption of the mouse Aga gene in embryonic stem cells, mice completely lacking Aga activity (Aga-/-) were generated (35). Heterozygote mating produced the expected Mendelian ratio of wild type, heterozygotes and homozygotes. In Aga-/- mice the natural substrate aspartylglucosamine accumulated in the brain and liver and was excreted in the urine. The mice did not exhibit clearly detectable phenotype and were fertile. At 5 months, however, Aga-/- mice showed gradual loss of motor coordination or balance and general appearance gradually deteriorated. Massively dilated urinary bladder (neurogenic?) was detected in mice at 10 months. As noted in human patients, vacuolation of cells in the CNS and visceral organs was conspicuous pathology of Aga-/- mice. Kupffer cells in the liver and glomeruli and proximal renal tubules were severely affected. In the brain, vacuolation of neurons, endothelial cells and glial cells were found. In addition axonal spheroids were noted in the gracile nuclei in the medulla and spinal cord. Thus, Aga-/- mice are phenotypically and pathologically very similar to human disease.

Therapeutic manipulations

Small animal models have definite advantages for testing therapeutic strategies for genetic diseases. Two naturally occurring murine models of lysosomal disease, twitcher and mucopolysaccharidosis VII have been widely used for such studies (32, 59, 94, 95). Zhou and co-workers (97) reported successful correction of clinical phenotype and systemic pathology in the PPCA-/- mice with transplantation of bone marrow that was derived from transgenic mice over expressing human protective protein precursor gene in the erythroid lineage cells under the control of the β-globin promotor and locus control region of the β-globin gene(23). Miranda and co-workers have been testing various parameters that are potentially highly influential for the outcome of bone marrow transplantation therapy, using

ASMKO mice (45). Using *Hexa*-/- mice, Platt and coworkers reported successful prevention of ganglioside accumulation by oral administration of an inhibitor of glycosphingolipid biosynthesis, N-butyldeoxynojirimycin (57). It has been reported that syngeneic bone marrow transplantation with wild-type bone marrow increased the life-span and improved neurologic symptoms in *Hexb*-/- mice (50). These reports indicate usefulness of knockout mice for exploration of therapeutic strategies for the lysosomal diseases.

Future directions

As described, nearly all human sphingolipidoses, three mucopolysaccharidoses and aspartylglucosaminuria exist spontaneously or have been duplicated in a directed fashion in mice. Undoubtedly mouse models of other human lysosomal disorders will be generated in the near future and new methodologies to insert precise human disease mutations into ES cells will allow the establishment of more accurate disease models. Genetic manipulation by cross-breeding among disease models or with other mutant mice is at the beginning phase, which should bring insight into the pathogenetic mechanism of these disorders unattainable with other means as has already been demonstrated by the double-knockout of the α- and β-subunits of β-hexosaminidase. However, many of the induced mutants have not been extensively explored for their potential as models of human lysosomal diseases beyond the basic characterization. Genetically authentic mouse models can overcome many of the scientific disadvantages in working with human patients. Often overlooked but in fact very important is that these mice can be bred to a homogeneous genetic background which can never be achieved in human population. Consequences of complex interactions among different genes in these disorders are being recognized in increasing frequency (42, 43). Then, one can do well-controlled experiments with sufficient numbers of normal, carrier and affected animals with relative ease. Experimental manipulations that are not allowed in human patients can be done with mice, including germline genetic manipulation. Extensive use of these mouse models for gene therapy attempts can be predicted in the near future. The results will be "cleaner" and the conclusions more reliable than patient studies. There is no room for anecdotal cases which so often clutter clinical studies and obscure the true logical conclusions or lack thereof. For strictly scientific inquiries into how nature works, the mouse models provide much better vehicles. On the other hand, if the ultimate aim is to understand and treat human diseases, it is equally important that we always keep in mind the simple and obvious dictum; "Mouse is not human". Even though the mouse models are useful and even though some other models in larger animals including monkeys (40) can fill the gap to some extent, studies on human patients are indispensable for pragmatic investigations. Animal experiments and human studies are complementary and both are needed.

Acknowledgement

This work has been supported in part by research grants RO1-NS24453, RO1-NS24289 and a Mental Retardation Research Center Core Grant P30-HD03110 from the USPHS

References

1. Alroy J, Orgad U, DeGasperi R, Richard R, Warren K, Knowles JG, Thalhammer JG, Raghavan SS (1992) Canine GM1-gangliosidosis: a clinical, morphologic, histochemical and biochemical comparison of two different models. *Am J Pathol* 140: 675-689
2. Alroy J, Warren CD, Raghavan SS, Kolodny EH (1989) Animal models for lysosomal storage diseases: Their past and future contribution. *Hum Pathol* 20: 823-826
3. Baker HJ, Mole JA, Linsey JR, Creel RM (1982) Animal models of human ganglioside storage diseases. *Fed Proc* 35: 1193-1201
4. Bapat B, Ethier M, Neote K, Mahuran D, Gravel RA (1988) Cloning and sequence of a cDNA encoding the β subunit of mouse β-hexosaminidase. *FEBS Lett* 237: 191-195
5. Beutler E, Grabowski GA (1995) Gaucher Disease. In: Metabolic and Molecular Basis of Inherited Disease, 7th Edition, Scriver CR, Beaudet AL, Sly WS, Valle D (eds.), Chapter 86, pp. 2641-2670, McGraw-Hill: New York.
6. Beccari T, Hoade J, Oriacchio J, Stirling JL (1992) Cloning and sequence analysis of a cDNA encoding the α subunit of mouse β-N-acetylhexosaminidase and comparison with the human enzyme. *Biochem J* 285: 593-596
7. Birkenmeier EH, Davisson MT, Beamer WG, Ganschow RE, Vogler CA, Gwynn B, Lyford KA, Maltais LM, Wawrzyniak CJ (1989) Murine mucopolysaccharidosis type VII. Characterization of a mouse with β-glucuronidase deficiency. *J Clin Invest* 83: 1258-1266
8. Boustany RM, Qian WH, Suzuki K (1993) Mutations in the lysosomal β-galactosidase cause GM1 gangliosidosis in American patients. *Am J Hum Genet* 53: 881-888
9. Bradova F, Ulrich-Bott B, Roggendorf W, Paton BC, Harzer K (1993) Prosaposin deficiency: Further characterization of the sphingolipid activator protein-deficient sibs. Multiple glycolipid elevations (including lactosylceramidosis), partial enzyme deficiencies and ultrastructure of the skin in this generalized sphingolipid storage disease. *Hum Genet* 92: 143-152

10. Burg J, Banerjee A, Conzelmann E, Sandhoff K (1983) Activating protein for ganglioside G_{M2} degradation by β-hexosaminidase isoenzymes in tissue extracts from different species. *Hoppe-Seyler Z Physiol Chem* 364: 821-829
11. Chakraborty S, Rafi MA, Wenger DA (1994) Mutations in the lysosomal β-galactosidase gene that cause the adult form of GM1-gangliosidosis. *Am J Hum Genet* 54: 1004-1013
12. Clarke LA, Russell CS, Pownall S, Warrington CL, Borowski A, Dimmick JE, Toone J, Jirik FR (1997) Murine mucopolysaccharidosis type I: targeted disruption of the murine α-L-iduronidase gene. *Hum Mol Genet* 6: 503-511
13. Cohen-Tannoudji M, Marchand P, Akli S, Sheardown SA, Puech J-P, Kress C, Gressens P, Nassogne M-C, Beccari T, Muggleton-Harris AL, Evrard P, Stirling JL, Poenaru L, Babinet C (1995) Disruption of murine *HEXA* gene leads to enzymatic deficiency and to neuronal lysosomal storage, similar to that observed in Tay-Sachs disease. *Mam Genome* 6: 844-849
14. d'Azzo A, Andrea G, Strisciuglio P, Galjaard H (1995) Galactosialidosis. In: The Metabolic and Molecular Basis of Inherited Disease, 7th Edition., Scriver CR, Beaudet AL, Sly WS, Valle D (eds.), Chapter 91, pp. 2825-2838, McGraw-Hill: New York.
15. Desnick RJ, Ioannou YA, Eng CM (1995) α-Galactosidase A deficiency: Fabry disease. In : The Metabolic and Molecular Basis of Inherited Disease, 7th Edition, Scriver CR, Beaudet AL, Sly WS, Valle D (eds.), Chapter 89, pp. 2741-2784, McGraw-Hill: New York
16. de Veber GA, Schwarting GA, Kolodny EH, Kowall NW (1992) Fabry disease. Immunochemical characterization of neuronal involvement. *Ann Neurol* 31: 409-415
17. Di Natale P, Annella T, Daniele A, Spagnuolo G, Cerundolo R, De Caprariis D, Gravino AE (1992) Animal models for lysosomal storage disease: a new case of feline mucopolysaccharidosis VI. *J Inher Metab Dis* 15: 17-24
18. Evers M, Saftig P, Schmidt P, Hafner A, McLoghlin DB, Schmahl WS, Hess B, von Figura K, Peters C (1996) Targeted disruption of the arylsulfatase B gene results in mice resembling the phenotype of mucopolysaccharodosis VI. *Proc Natl Acad Sci USA* 93: 8214-8219
19. Fujita N, Suzuki K, Vanier M, Popko B, Maeda N, Klein A, Henseler M, Sandhoff K, Nakayasu H, Suzuki K (1996) Targeted disruption of the mouse sphingolipid activator protein gene: a complex phenotype, including severe leukodystrophy and wide-spread storage of multiple sphingolipids. *Hum Mol Genet* 5: 711-725
20. Gieselmann V, Zlotogora J, Harris A, Wenger DA, Morris CP (1994) Molecular genetics of metachromatic leukodystrophy. *Hum Mutat* 4: 233-242
21. Gravel RA, Clark JTR, Kaback MN, Mahuran D, Sandhoff K, Suzuki K (1995) The G_{M2} gangliosidosis. In : The Metabolic and Molecular Basis of Inherited Disease, 7th Edition, Scriver CR, Beaudet AL, Sly WS, Valle D (eds.), Chapter 92, pp. 2839-2879, McGraw-Hill: New York
22. Gregoire A, Perier O, Dustin P (1966) Metachromatic leukodystrophy, an electron microscopic study. *J Neuropathol Exp Neurol* 25: 617-636
23. Grosveld F, van Assendelft G B, Greaves DR, Kollias G (1987) Position-independent, high level expression of the human β-globin gene in transgenic mice. *Cell* 51: 975-985.
24. Hahn CN, del Pilar Martin M, Schröder M, Vanier MT, Hara Y, Suzuki K, Suzuki K, d'Azzo A. (1997) Generalized CNS disease and massive GM1-ganglioside accumulation in mice defective in lysosomal acid β-galactosidase. *Hum Mol Genet* 6: 205-211
25. Harzer K, Paton BC, Poulos A, Kustermann-Kuhn B, Roggendorf W, Grisar T, Popp M (1989) Sphingolipid activator deficiency in a 16 week old atypical Gaucher disease patient and his fetal sibling: Biochemical signs of combined sphingolipidoses. *Eur J Pediatr* 149: 31-39
26. Haskins M, Baker HJ, Birkenmeier E, Hoogerbrugge P, Poorthuis B, Sakiyama T, Shull R, Taylor RM, Thrall M, Walkley SU (1991) Transplantation in animal model systems. In: Treatment of genetic diseases. Desnick RJ (ed.), pp. 183-201, Churchill Livingstone: Edinburgh, London
27. Haskins ME, Desnick RJ, DiFerrante N, Jezyik PF, Patterson DF (1984) β-glucuronidase deficiency in a dog. A model of human mucopolysaccharidosis VII. *Pediatr Res* 18: 980-984
28. Haskins ME, Jezyk PF, Desnick RJ, McDonough SK, Patterson DF (1979) α -L-iduronidase deficiency in a cat: A model of mucopolysaccharidoses I. *Pediatr Res* 13: 1294-1297
29. Hess B, Saftig P, Hartmann D, Coenen R, Lüllmann-Rauch R, Goebel HH, Evers M, von Figura K, D'Hooge R, Nagels G, De Deyn P, Peters C, Gieselmann V (1996) Phenotype of arylsulfatase A-deficient mice: relationship to human metachromatic leukodystrophy. *Proc Natl Acad Sci USA* 93: 14821-14828
30. Ho MW, O'Brien JS (1971) Gaucher's disease: deficiency of "acid" β-glucosidase and reconstitution of enzyme activity in vitro. *Proc Natl Acad Sci USA* 68: 2810-2813
31. Holleran WM, Ginns EI, Menon GK, Grundmann J-U, Fartasch M, McKinney CE, Elias PM, Sidransky E. (1994) Consequences of β-glucocerebrosidase deficiency in epidermis : ultrastructure and permeability barrier alteration in Gaucher disease. *J Clin Invest* 91: 1736-1764
32. Hoogerbrugge PM, Suzuki K, Suzuki K, Poorthuis BJHM, Kobayashi T, Wagemaker G, van Bekkum DW (1988) Donor derived cells in the central nervous system of twitcher mice after bone marrow transplantation. *Science* 239: 1035-1038
33. Horinouchi K, Erlich S, Perl DP, Ferlinz K, Bisgaier CL, Sandhoff K, Desnick RJ, Stewart CL, Schuchman EH (1995) Acid sphingomyelinase deficient mice: a model of type A and B Niemann-Pick disease. *Nature Genet* 10: 288-293
34. Jezyk PF, Haskins ME, Patterson DF, Mellman WJ, Greenstein M (1977) Mucopolysaccharidosis in a cat with arylsulfatase B deficiency. A model of Maroteaux-Lamy syndrome. *Science* 198: 834-836
35. Kaartinen V, Mononen I, Voncken JW, Noronkoski T, Gonzalez-Gomez, Heisterkamp N and Groffen J (1996) A mouse model for the human lysosomal disease aspartylglucosaminuria. *Nature Med* 2: 1375-1378

36. Kolodny EH, Fluharty AL (1995) Metachromatic leukodystrophy and multiple sulfatase deficiency: sulfatide lipidosis. In: The Metabolic and Molecular Basis of Inherited Diseases, 7th Edition, Scriver CR, Beaudet AL, Sly WS, Valle D (eds.), Chapter 88, pp. 2693-2739, McGraw-Hill: New York

37. Kuemmel TA, Schroeder R, Stoffel W (1997) Light and electron microscopic analysis of the central and peripheral nervous systems of acid sphingomyelinase-deficient mice resulting from gene targeting. *J Neuropathol Exp Neurol* 56: 171-179

38. Leinekugel P, Michel S, Conzelmann E, Sandhoff K (1992) Quantitative correlation between the residual activity of β-hexosaminidase A and arylsulfatase A and the severity of the resulting lysosomal storage disease. *Hum Genet* 88: 513-523

39. Liu Y, Hoffmann A, Grinberg A, Westphal H, McDonald MP, Miller KM, Crawley JN, Sandhoff K, Suzuki K, Proia RL (1997) Mouse model of GM2 activator deficiency manifests cerebellar pathology and motor impairment. *Proc Natl Acad Sci USA* 94: 8138-8143

40. Luzi P, Rafi MA, Victoria T, Baskin GB, Wenger DA (1997) Characterization of the rhesus monkey galactocerebrosidase (GALC) cDNA and gene and identification of the mutation causing globoid cell leukodystrophy (Krabbe disaes) in the primate. *Genomics* 42: 319-324

41. Matsuda J, Suzuki O, Oshima A, Ogura A, Naiki M, Suzuki Y (1997) Neurological manifestations of knockout mice with b-galactosidase deficiency. *Brain Dev* 19: 19-20

42. Matsumoto A, Vanier MT, Oya Y, Kelly D, Popko B, Wenger DA, Suzuki K, Suzuki K (1998) Minimal increment in galactosylceramidase expression is sufficient for significant phenotypic improvement in twitcher mouse. *Dev Brain Dysfunc*t, in press

43. Matsushima G, Taniike M, Glimcher LH, Grusby MJ, Frelinger JA, Suzuki K, Ting J P-Y (1994) Absence of MHC Class II molecules reduces CNS demyelination, microglial/macrophages infiltration, and twitching in murine globoid cell leukodystrophy. *Cell* 78: 645-656

44. Mehl E, Jatzkewitz H (1964) Eine Cerebrosidsulfatase aus Schweineniere. *Hoppe-Seylers Z Physiol Chem* 339: 260-276

45. Miranda SRP, Erlich S, Visser JWM, Gatt S, Dagan A, Friedrich VL Jr, Schuchman EH (1997) Bone marrow transplantation in acid sphingomyelinase-deficient mice: engraftment and cell migration into the brain as a function of radiation, age, and phenotype. *Blood* 90: 444-452

46. Muldoon LL, Neuwelt EA, Pagel MA, Weiss DL (1994) Characterization of the molecular defect in a feline model for type II G_{M2}-Gangliosidosis (Sandhoff Disease). *Am J Pathol* 144: 1109-1118

47. Neufeld EF, Muenzer J (1995) The Mucopolysaccharidoses In: The Metabolic and Molecular Basis of Inherited Diseases, 7th Edition, Scriver CR, Beaudet AL, Sly WS, Valle D (eds.), Chapter 78, pp. 2465-2494, McGraw-Hill: New York

48. Nishimoto J, Namba E, Inui K, Okada S, Suzuki K (1991) G_{M1} gangliosidosis (genetic β-galactosidase deficiency): identification of four mutations in different clinical phenotypes among Japanese patients. *Am J Hum Genet* 49: 566-574

49. Nordborg C, Kyllerman M, Conradi N, Mansson J-E (1997) Early-infantile galactosialidosis with multiple brain infarctions: morphological, neuropathological and neurochemical findings. *Acta Neuropathol (Berl)* 93: 24-33

50. Norflus FN, McDonald MP, Crawley JN, Suzuki K, Proia RL, Tifft CJ (1996) Bone marrow transplantation as a therapy for GM2 gangliosidosis. *Am J Hum Genet* 59: A204

51. Ohshima T, Murray GJ, Swaim WD, Longenecker G, Quirk JM, Cardarelli CO, Sugimoto Y, Pastan I, Gottesman MM, Brady RO, Kulkarni AB (1997) α-galactosidase A deficient mice: a model of Fabry disease. *Proc Natl Acad Sci USA* 94: 2540-2544

52. Otterbach B, Stoffel W (1995) Acid sphingomyelinase-deficient mice mimic the neurovisceral form of human lysosomal storage disease (Niemann-Pick disease). *Cell* 81: 1053-1061

53. Oya Y, Nakayasu H, Fujita N, Suzuki K, Suzuki K. Pathological study of mice with total deficiency of sphingolipid activator proteins (SAP knockout mice). *Acta Neuropathol (Berl)*, submitted

54. Oyanagi K, Ohama E, Miyashita K, Yoshino H, Miyatake T, Yamazaki M, Ikuta F (1991) Galactosialidosis: neuropathological findings in a case of the late infantile type. *Acta Neuropathol (Berl)* 82: 331-339

55. Peng L, Suzuki K (1987) Ultrastructural study of neurons in metachromatic leukodystrophy. *Clin Neuropathol* 6: 224-230

56. Phaneuf D, Wakamatsu N, Huang J-Q, Borowski A, Peterson AC, Fortunato SR, Ritter G, Igdoura SA, Morales CR, Benoit G, Akerman BR, Leclerc D, Hanai N, Martin JD, Trasler JM, Gravel RA. (1996) Dramatically different phenotypes in mouse models of human Tay-Sachs and Sandhoff diseases. *Hum Mol Genet* 5: 1-14

57. Platt FM, Neises GR, Reinkensmeier G, Townsend MJ, Perry VH, Proia R, Winchester B, Dwek RA, Butters TD (1997) Prevention of lysosomal storage in Tay-Sachs mice treated with N-Butyldeoxynojirimycin. *Science* 276: 428-431

58. Rahman AN, Lindenberg R. (1963) The neuropathology of hereditary dystrophic lipidosis. *Arch Neurol* 9: 373-385

59. Sands MS, Vogler C, Torrey A, Levy B, Gwynn B, Grubb J, Sly WS, Birkenmeier EH (1997) Murine mucopolysaccharidosis type VII: longterm therapeutic effects of enzyme replacement and enzyme replacement following by bone marrow transplantation. *J Clin Invest* 99: 1596-1605

60. Sango K, McDonald MP, Crawley JN, Mack ML, Tifft CJ, Skop E, Starr CM, Hoffmann A, Sandhoff K, Suzuki K, Proia RL. (1996) Mice lacking both subunits of lysosomal β-hexosaminidase display gangliosidosis and mucopolysaccharidosis. *Nature Genet* 14: 348-352

61. Sango K, Yamanaka S, Hoffmann A, Okuda Y, Grinberg A, Westphal H, McDonald MP, Crawley JN, Sandhoff K, Suzuki K, Proia RL. (1995) Mouse models of Tay-Sachs and Sandhoff diseases differ in neurologic phenotype and ganglioside metabolism. *Nature Genet* 11: 170-176

62. Sandhoff K, Harzer K, Fürst W (1995) Sphingolipid activator proteins In: The Metabolic and Molecular Basis of Inherited Diseases, 7th Edition, Scriver CR, Beaudet AL, Sly WS, Valle D (eds.), Chapter 76, pp. 2427-2441, McGraw Hill: New York

63. Schnabel D, Schröder M, Fürst M, Klein A, Hurwitz R, Zenk T, Weber J, Harzer K, Paton BC, Poulos A, Suzuki K, Sandhoff K (1992) Simultaneous deficiency of sphingolipid activator proteins 1 and 2 is caused by a mutation in the initiation codon of their common gene. J Biol Chem 267: 3312-3315

64. Schuchman EH, Desnick RJ (1995) Niemann-Pick disease type A and B: acid sphingomyelinase deficiencies. In: The Metabolic and Molecular Basis of Inherited Diseases, 7th Edition, Scriver CR, Beaudet AL, Sly WS, Valle D (eds.), Chapter 84, pp. 2601-2624, McGraw-Hill: New York

65. Scott HS, Bunge S, Gal A, Clarke LA, Morris CP, Hopwood JJ (1995) Molecular genetics of mucopolysaccharidosis type I: diagnostic, clinical and biological implications. *Hum Mutat* 6: 288-302

66. Shull RM, Helman RG, Spellacy E, Constantopoulos G, Munger RJ, Neufeld EF (1984) Morphologic and biochemical studies of canine mucopolysaccharidosis I. *Am J Pathol* 114: 487-495

67. Sidransky E, Fartasch M, Lee RE, Metlay LA, Abella S, Zimran A, Gao W, Elias PM, Ginns EI, Holleran WM (1996) Epidermal abnormalities may distinguish type 2 from type 1 and 3 of Gaucher disease. *Pediatr Res* 39: 134-141

68. Sidransky E, Sherer DM, Ginns EI (1992) Gaucher disease in the neonate: A distinct Gaucher phenotype is analogous to a mouse model created by targeted disruption of the glucocerebrosidase gene. *Pediatr Res* 32: 494-498

69. Sung JH (1979) Autonomic neurons affected by lipid storage in the spinal cord in Fabry's disease: distribution of autonomic neurons in the sacral cord. *J Neuropathol Exp Neurol* 38: 87-98

70. Suzuki K (1968) Cerebral GM1-gangliosidosis: chemical pathology of visceral organs. *Science* 159: 1471-1472

71. Suzuki K (1991) Neuropathology of late onset gangliosidosis: a review. *Dev Neurosci* 13: 205-210

72. Suzuki K (1994) A genetic demyelinating disease globoid cell leukodystrophy: studies with animal models. J Neuropath *Exp Neurol* 53: 359-363

73. Suzuki K, Sango K, Proia RL, Langaman CL (1997) Mice deficient in all forms of lysosomal β-hexosaminidase show mucopolysaccharidosis-like pathology. J Neuropathol *Exp Neurol* 56: 693-703

74. Suzuki K, Suzuki K (1996) The gangliosidoses. In: Handbook of Clinical Neurology, Vinken PJ, Bruyn GW (eds.) Vol 66, revised Series 22: Neurodystrophies and Neurolipidoses, Moser H (volume ed.), pp. 247-280, Elsevier Science Publishers: Amsterdam

75. Suzuki Y, Oshima A (1993) A β-galactosidase gene mutation identified in both Morquio B disease and infantile G_{M1}-gangliosidosis. *Hum Genet* 91: 407

76. Suzuki Y, Sakuraba H, Oshima A (1995) β-galactosidase deficiency (β-galactosidosis): GM1 gangliosidosis and Morquio B disease. In: The Metabolic and Molecular Basis of Inherited Disease, 7th Edition, Scriver CR, Beaudet AL, Sly WS, Valle D (eds.), Chapter 90, pp. 2785-2824, McGraw-Hill: New York

77. Taniike M, Yamanaka S, Proia RL, Langaman CL, Bone-Turrentine T, Suzuki K (1995) Neuropathology of mice with targeted disruption of *Hexa* gene, a model of Tay-Sachs disease. *Acta Neuropathol (Berl)* 89: 296-304

78. Terry RD, Korey SR (1960) Membranous cytoplasmic granules in infantile amaurotic idiocy *Nature* 188: 1000-1002

79. Terry RD, Weiss M (1963) Studies in Tay-Sachs disease: II. Ultrastructure of cerebrum. *J Neuropathol Exp Neurol* 22:18-55

80. Thomas GH, Beaudet AL (1995) Disorders of glycoprotein degradation and structure: α-mannosidosis, β-mannosidosis, fucosidosis, scialidosis, aspartylglucosaminuria, and carbohydrate-deficient glycoprotein syndrome. In: The Metabolic and Molecular Basis of Inherited Disease, 7th Edition, Scriver CR, Beaudet AL, Sly WS, Valle D (eds.), Chapter 81, pp. 2529-2561, McGraw-Hill: New York

81. Thompson JN, Jones MZ, Dawson G, Huffman PS (1992) N-acetylglucosamine 6 sulfatase deficiency in a Nubian goat: A model of Sanfilippo syndrome type D (mucopolysaccharidosis IIID) *J Inher Metab Dis* 15: 760-768

82. Tybulewicz VLJ, Tremblay ML, LaMarca ME, Willemsen RW, Stubblefield BK, Winfield S, Zablocka B, Sidransky E, Martin BM, Huang SP, Mintzer KA, Westphal H, Mulligan RC, Ginns EI (1992) Animal model of Gaucher's disease from targeted disruption of the mouse glucocerebrosidase gene. *Nature* 357: 407-410

83. Vanier MT, Suzuki K (1996) Niemann-Pick disease. In: Handbook of Clinical Neurology, Vinken PJ, Bruyn GW (eds.), Vol. 66, revised Series 22: Neurodystrophies and Neurolipidoses, Moser H (volume ed.), pp. 133-162, Elsevier Science Publishers: Amsterdam

84. Von Hirsch T, Peiffer J (1955) Über histologische Methoden in der Differentialdiagnose von Leukodystrophien und Lipidosen. *Arch Psychiatr Nervenkr* 194: 88-104

85. Walkley SU (1988) Pathobiology of neuronal storage disease. *Int Rev Neurobiol* 29: 191-244

86. Walkley SU, Thrall MA, Dobrenis K, Huang M, March PA, Siegel DA, Wurzelmann S (1994) Bone marrow transplantation corrects the enzyme defect in neurons of the central nervous system in a lysosomal storage disease. *Proc Natl Acad Sci USA* 91: 2970-2974

87. Wang AM, Stewart CL, Desnick RJ (1993) α-N-Acetylgalactosaminidase: characterization of the murine cDNA and genomic sequences and generation of the mice by targeted gene disruption. (abstract). *Am J Hum Genet* 53: 99

88. Wenger DA, Tarby TJ, Wharton C (1978) Macular cherry-red spots and myoclonus with dementia: Coexistent neuraminidase and β-galactosidase deficiencies. Biochem *Biophys Res Commun* 82: 589-595

89. Willemsen R, Tybulewicz E, Sidransky E, Eliason WK, Martin BM, LaMarca ME, Reuser AJJ, Tremblay M, Westphal H, Mulligan RC, Ginns EI (1995) A biochemical and ultrastructural evaluation of the type 2 Gaucher mouse. *Mol Chem Neuropathol* 24: 179-192

90. Wolf HJ, Pietra GG (1964) The visceral lesions of metachromatic leukodystrophy. *Am J Pathol* 44: 921-930

91. Yamanaka S, Johnson MD, Grinberg A, Westphal H, Crawley JN, Taniike M, Suzuki K, Proia RL (1994) Targeted disruption of the *Hexa* gene results in mice with biochemical and pathologic features of Tay-Sachs disease. *Proc Natl Acad Sci USA* 91: 9975-9979

92. Yamanaka S, Johnson ON, Norflus F, Boles DJ, Proia RL (1994) Structure and expression of the mouse β-hexosaminidase genes, *Hexa* and *Hexb*. *Genomics* 21: 588-596

93. Yamano T, Shimada M, Sugino H, Dezawa T, Koike M, Okada S, Yabuuchi H (1985) Ultrastructural study on a severe infantile sialidosis (β-galactosidase-α-neuraminidase deficiency). *Neuropediatrics* 16: 109-112

94. Yeager AM, Brennan S, Tiffany C, Moser HW, Santos CW (1984) Prolonged survival and remyelination after hematopoietic cell transplantation in the twitcher mouse. *Science* 225: 1052-1054

95. Yeager AM, Shinn C, Shinohara M, Pardoll DM (1993) Hematopoietic cell transplantation in the twitcher mouse: The effects of pretransplant conditioning with graded doses of Busulfan. *Transplantation* 56: 185-190

96. Yoshida M, Ikadai A, Maekawa A, Takahashi M, Nagase S (1993) Pathological characteristics of mucopolysaccharidosis VI in the rat. *J Comp Pathol* 109 :141-153

97. Zhou XY, Morreau H, Rottier R, Davis D, Bonten E, Gillemans N, Wenger D, Grosveld FG, Doberty P, Suzuki K, Grosveld GC, d'Azzo A (1995) Mouse model for the lysosomal disorder galactosialidosis and correction of the phenotype with overexpressing erythroid precursor cells. *Genes Dev* 9: 2623-2634